Buckling Behavior of Long Symmetrically Laminated Plates Subjected to Shear and Linearly Varying Axial Edge Loads

Michael P. Nemeth
Langley Research Center • Hampton, Virginia

Available electronically at the following URL address: http://techreports.larc.nasa.gov/ltrs/ltrs.html

Printed copies available from the following:

Abstract

A parametric study of the buckling behavior of infinitely long symmetrically laminated anisotropic plates that are subjected to linearly varying edge loads, uniform shear loads, or combinations of these loads is presented. The study focuses on the effects of the shape of linearly varying edge load distribution, plate orthotropy, and plate flexural anisotropy on plate buckling behavior. In addition, the study examines the interaction of linearly varying edge loads and uniform shear loads with plate flexural anisotropy and orthotropy. Results obtained by using a special purpose non-dimensional analysis that is well suited for parametric studies of clamped and simply supported plates are presented for [±θ]ₛ thin graphite-epoxy laminates that are representative of spacecraft structural components. Also, numerous generic buckling-design charts are presented for a wide range of nondimensional parameters that are applicable to a broad class of laminate constructions. These charts show explicitly the effects of flexural orthotropy and flexural anisotropy on plate buckling behavior for linearly varying edge loads, uniform shear loads, or combinations of these loads. The most important finding of the present study is that specially orthotropic and flexurally anisotropic plates that are subjected to an axial edge load distribution that is tension dominated can support shear loads that are larger in magnitude than the shear buckling load.

Introduction

Buckling behavior of laminated plates that are subjected to combined loads is an important consideration in the preliminary design of aircraft and launch vehicles. The sizing of many structural subcomponents of these vehicles is often determined by stability constraints. One subcomponent that is of practical importance in structural design is the long rectangular plate. These plates commonly appear as subcomponents of stiffened panels used for wing structures and as semimonocoque shell segments used for fuselage and launch vehicle structures. Buckling results for infinitely long plates are important because they often provide a useful conservative estimate of the behavior of finite-length rectangular plates, and they provide information that is useful in explaining the behavior of these finite-length plates. Moreover, knowledge of the behavior of infinitely long plates can provide insight into the buckling behavior of more complex structures such as stiffened panels.

An important type of long plate that appears as a subcomponent of advanced composite structures is the symmetrically laminated plate. In the present paper, the term "symmetrically laminated" refers to plates in which every lamina above the plate midplane has a corresponding lamina located at the same distance below the plate midplane, with the same thickness, material properties, and fiber orientation. Symmetrically laminated plates remain flat during the manufacturing process and exhibit flat prebuckling deformation states. These characteristics and the amenability of these plates to structural tailoring provide symmetrically laminated plates with a significant potential for reducing structural weight of aircraft and launch vehicles. Thus, understanding the buckling behavior of symmetrically laminated plates is an important part of the search for ways to exploit plate orthotropy and anisotropy to reduce structural weight.

In many practical cases, symmetrically laminated plates exhibit specially orthotropic behavior. However, in some cases, such as [±45]ₛ laminates, these plates exhibit anisotropy in the form of material-induced coupling between pure bending and twisting deformations. This coupling is referred to herein as flexural anisotropy, and it generally yields buckling modes that are skewed in appearance. The effects of flexural orthotropy and flexural anisotropy on the buckling behavior of long rectangular plates that are subjected to single and combined loading conditions are becoming better understood. For example, recent in-depth parametric studies that show the effects of anisotropy on the buckling behavior of long plates that are subjected to compression, shear, pure in-plane bending, and various combinations of these loads have been presented in references 1 through 5. The results presented in these references indicate that the importance of flexural anisotropy on the buckling resistance of long plates varies with the magnitude and type of the combined loading condition. However, none of these studies supply results for plates loaded by uniform shear and a general linear distribution of axial load across the plate width. Both the uniform axial compression and the pure in-plane bending loads are special cases of the general linear distribution of axial edge loads. Results for this class of loadings are useful in the design of aircraft spar webs and panels that are located off the neutral axis of a fuselage or launch vehicle that is subjected to overall bending and torsion loads. Moreover, the importance of neglecting flexural anisotropy in a buckling analysis is practically unknown for this class of loadings.

One objective of the present paper is to present buckling results for specially orthotropic plates that are subjected to uniform shear, a general linear distribution of axial load across the plate width, and combinations of these loads in terms of useful nondimensional design parameters. Other objectives are to identify the effects of flexural anisotropy on the buckling behavior of long symmetrically laminated plates that are subjected to the same loading conditions and to present some previously unknown results that show some unusual behavior. Results are presented for plates with the two long edges clamped or simply supported and that are free to move in their plane. Several generic buckling-design curves that are applicable to a wide range of laminate constructions are also presented in terms of the nondimensional parameters described in references 1, 2, 5, and 6.

Symbols

A_m, B_m	displacement amplitudes (see eq. (22)), in.
b	plate width (see fig. 1), in.
$D_{11}, D_{12}, D_{22}, D_{66}$	orthotropic plate-bending stiffnesses, in-lb
D_{16}, D_{26}	anisotropic plate-bending stiffnesses, in-lb
E_1, E_2, G_{12}	lamina moduli, psi
$K_b \equiv (n_{b1})_{cr}$	nondimensional buckling coefficient associated with critical value of an eccentric in-plane bending load (see eq. (21) and fig. 1(a))
$K_s \equiv (n_{xy1})_{cr}$	nondimensional buckling coefficient associated with critical value of a uniform shear load (see eq. (20) and fig. 1(a))
$K_s\big|_{\gamma=\delta=0}, K_b\big|_{\gamma=\delta=0}$	shear and in-plane bending buckling coefficients, defined by equations (20) and (21), respectively, in which anisotropy is neglected in the analysis
$K_x \equiv (n_{x1}^c)_{cr}$	nondimensional buckling coefficient associated with critical value of a uniform axial compression load (see eq. (18) and fig. 1(a))
$K_y \equiv (n_{y1})_{cr}$	nondimensional buckling coefficient associated with critical value of a uniform transverse compression load (see eq. (19) and fig. 1(a))
L_1, L_2, L_3, L_4	nondimensional load factors defined by equations (14) through (17), respectively
$n_{x1}^c, n_{y1}, n_{xy1}, n_{b1}$	nondimensional membrane stress resultants of system of destabilizing loads defined by equations (10) through (13), respectively
$n_{x2}^c, n_{y2}, n_{xy2}, n_{b2}$	nondimensional membrane stress resultants of system of subcritical loads defined by equations (10) through (13), respectively
N	number of terms in series representation of out-of-plane displacement field at buckling (see eq. (22))
N_b	intensity of eccentric in-plane bending load distribution defined by equation (5), lb/in.
N_{xc}	intensity of constant-valued tension or compression load distribution defined by equation (5), lb/in.
N_x, N_y, N_{xy}	longitudinal, transverse, and shear membrane stress resultants, respectively (see eqs. (5), (7), and (8)), lb/in.
$N_{x1}^c, N_{y1}, N_{xy1}, N_{b1}$	membrane stress resultants of system of destabilizing loads (see eqs. (6) through (9)), lb/in.
$N_{x2}^c, N_{y2}, N_{xy2}, N_{b2}$	membrane stress resultants of system of subcritical loads (see eqs. (6) through (9)), lb/in.
$\tilde{p}, \tilde{p}_{cr}$	nondimensional loading parameter (see eqs. (14) through (17)) and corresponding value at buckling (see eqs. (18) through (21)), respectively
$w_N(\xi, \eta)$	out-of-plane displacement field at buckling defined by equation (22), in.
x, y	plate rectangular coordinate system (see fig. 1), in.
$\alpha_\infty, \beta, \gamma, \delta$	nondimensional parameters defined by equations (1), (2), (3), and (4), respectively
$\varepsilon_0, \varepsilon_1$	in-plane bending load distribution parameters (see fig. 1 and eq. (5))

$\eta = y/b, \xi = x/\lambda$ nondimensional plate coordinates

θ fiber angle of a lamina (see fig. 1), deg

λ half-wavelength of buckling mode (see fig. 1), in.

λ/b buckle aspect ratio (see fig. 1)

ν_{12} lamina major Poisson's ratio

$\Phi_m(\eta)$ basis functions used to represent buckling mode (see eq. (22))

Analysis Description

In preparing generic design charts for buckling of a single flat plate, a special purpose analysis is often preferred over a general purpose analysis code, such as a finite element code, because of the cost and effort usually involved in generating a large number of results with a general purpose code. The results presented herein were obtained by using such a special purpose analysis. The analysis details are lengthy; hence, only a brief description of the analysis is presented.

Symmetrically laminated plates can have many different constructions because of the wide variety of material systems, fiber orientations, and stacking sequences that can be used to construct a laminate. A way of coping with the vast diversity of laminate constructions is to use convenient nondimensional parameters. The buckling analysis used in the present paper is based on classical plate theory and the classical Rayleigh-Ritz method and was derived explicitly in terms of the nondimensional parameters defined in references 1, 2, 5, and 6. This approach was motivated by the need for generic (independent of laminate construction) parametric results for composite plate buckling behavior that are expressed in terms of the minimum number of independent parameters needed to fully characterize the behavior and that indicate the overall trends and sensitivity of the results to changes in the parameters. The nondimensional parameters used in the present paper are given by

$$\alpha_\infty = \frac{b}{\lambda}\left(\frac{D_{11}}{D_{22}}\right)^{1/4} \tag{1}$$

$$\beta = \frac{D_{12} + 2D_{66}}{(D_{11}D_{22})^{1/2}} \tag{2}$$

$$\gamma = \frac{D_{16}}{(D_{11}^3 D_{22})^{1/4}} \tag{3}$$

$$\delta = \frac{D_{26}}{(D_{11}D_{22}^3)^{1/4}} \tag{4}$$

where b is the plate width and λ is the half-wavelength of the buckle pattern of an infinitely long plate (see fig. 1). The subscripted D-terms are the bending stiffnesses of classical laminated plate theory. The parameters α_∞ and β characterize the flexural orthotropy, and the parameters γ and δ characterize the flexural anisotropy.

The loading combinations included in the analysis are uniform transverse tension or compression, uniform shear, and a general linear distribution of axial load across the plate width, as depicted in figure 1. The longitudinal stress resultant N_x is partitioned in the analysis into a uniform tension or compression part and a linearly varying part corresponding to eccentric in-plane bending loads. This partitioning is given by

$$N_x = N_{xc} - N_b[\varepsilon_0 + (\varepsilon_1 - \varepsilon_0)\eta] \tag{5}$$

where N_{xc} denotes the intensity of the constant-valued tension or compression part of the load, and the term containing N_b defines the intensity of the eccentric in-plane bending load distribution. The symbols ε_0 and ε_1 define the distribution of the in-plane bending load, and the symbol η is the nondimensional coordinate given by $\eta = y/b$ (see fig. 1).

The analysis is based on a general formulation that includes combined destabilizing loads that are proportional to a positive-valued loading parameter $\bar{p}$ that is increased until buckling occurs and independent subcritical combined loads that remain fixed at a specified load level below the value of the buckling load. Herein, the term "subcritical load" is defined as any load that does not cause buckling to occur. In practice, the subcritical loads are applied to a plate prior to the destabilizing loads with an intensity below that which will cause the plate to buckle. Then, with the subcritical loads fixed, the destabilizing loads are applied by increasing the magnitude of the loading parameter until buckling occurs. This approach permits certain types of combined load interaction to be investigated in a direct and convenient manner.

The distinction between the destabilizing and subcritical loading systems is implemented in the buckling analysis by partitioning the prebuckling stress resultants as follows:

$$N_{xc} = -N_{x1}^c + N_{x2}^c \tag{6}$$

$$N_y = -N_{y1} + N_{y2} \tag{7}$$

$$N_{xy} = N_{xy1} + N_{xy2} \tag{8}$$

$$N_b = N_{b1} + N_{b2} \qquad (9)$$

where the stress resultants with the subscript 1 are the destabilizing loads, and those with the subscript 2 are the subcritical loads. The sign convention used herein for positive values of these stress resultants is shown in figure 1. In particular, positive values of the general linear edge stress distribution parameters N_{b1}, N_{b2}, ε_0, and ε_1 correspond to compression loading. Negative values of N_{b1} and N_{b2}, or negative values of either ε_0 or ε_1 yield linearly varying stress distributions that include tension. The two normal stress resultants of the system of destabilizing loads, N_{x1}^c and N_{y1}, are defined as positive valued for compression loads. This convention results in positive eigenvalues being used to indicate instability caused by uniform compression loads.

The buckling analysis includes several nondimensional stress resultants associated with equations (6) through (9). These dimensionless stress resultants are given by

$$n_{xj}^c = \frac{N_{xj}^c b^2}{\pi^2 (D_{11} D_{22})^{1/2}} \qquad (10)$$

$$n_{yj} = \frac{N_{yj} b^2}{\pi^2 D_{22}} \qquad (11)$$

$$n_{xyj} = \frac{N_{xyj} b^2}{\pi^2 (D_{11} D_{22}^3)^{1/4}} \qquad (12)$$

$$n_{bj} = \frac{N_{bj} b^2}{\pi^2 (D_{11} D_{22})^{1/2}} \qquad (13)$$

where the subscript j takes on the values of 1 and 2. In addition, the destabilizing loads are expressed in terms of the loading parameter $\tilde{p}$ in the analysis by

$$n_{x1}^c = L_1 \tilde{p} \qquad (14)$$

$$n_{y1} = L_2 \tilde{p} \qquad (15)$$

$$n_{xy1} = L_3 \tilde{p} \qquad (16)$$

$$n_{b1} = L_4 \tilde{p} \qquad (17)$$

where L_1 through L_4 are load factors that determine the specific form (relative magnitude of the load components) of a given system of destabilizing loads. Typically, the dominant load factor is assigned a value of 1, and all others are given as positive or negative fractions.

Nondimensional buckling coefficients used herein are given by the values of the dimensionless stress resultants of the system of destabilizing loads at the onset of buckling; that is,

$$K_x \equiv (n_{x1}^c)_{cr} = \frac{(N_{x1}^c)_{cr} b^2}{\pi^2 (D_{11} D_{22})^{1/2}} = L_1 \tilde{p}_{cr} \qquad (18)$$

$$K_y \equiv (n_{y1})_{cr} = \frac{(N_{y1})_{cr} b^2}{\pi^2 D_{22}} = L_2 \tilde{p}_{cr} \qquad (19)$$

$$K_s \equiv (n_{xy1})_{cr} = \frac{(N_{xy1})_{cr} b^2}{\pi^2 (D_{11} D_{22}^3)^{1/4}} = L_3 \tilde{p}_{cr} \qquad (20)$$

$$K_b \equiv (n_{b1})_{cr} = \frac{(N_{b1})_{cr} b^2}{\pi^2 (D_{11} D_{22})^{1/2}} = L_4 \tilde{p}_{cr} \qquad (21)$$

where $\tilde{p}_{cr}$ is the magnitude of the loading parameter at buckling. Positive values of the coefficients K_x and K_y correspond to uniform compression loads, and the coefficient K_s corresponds to uniform positive shear. The direction of a positive shear stress resultant acting on a plate is shown in figure 1. The coefficient K_b corresponds to the specific in-plane bending load distribution defined by the selected values of the parameters ε_0 and ε_1.

The mathematical expression used in the variational analysis to represent the general off-center and skewed buckle pattern is given by

$$w_N(\xi, \eta) = \sum_{m=1}^{N} (A_m \sin \pi\xi + B_m \cos \pi\xi) \Phi_m(\eta) \qquad (22)$$

where $\xi = x/\lambda$ and $\eta = y/b$ are nondimensional coordinates, w_N is the out-of-plane displacement field, and A_m and B_m are the unknown displacement amplitudes. In accordance with the Rayleigh-Ritz method, the basis functions $\Phi_m(\eta)$ are required to satisfy the kinematic boundary conditions on the plate edges at $\eta = 0$ and 1. For the simply supported plates, the basis functions used in the analysis are given by

$$\Phi_m(\eta) = \sin [m\pi\eta] \qquad (23)$$

for values of $m = 1, 2, 3, ..., N$. Similarly, for the clamped plates, the basis functions are given by

$$\Phi_m(\eta) = \cos [(m-1)\pi\eta] - \cos [(m+1)\pi\eta] \qquad (24)$$

For both boundary conditions, the two long edges of a plate are free to move in the x-y plane.

Algebraic equations governing the buckling behavior of infinitely long plates are obtained by substituting the series expansion for the buckling mode given by equation (22) into the second variation of the total potential energy and then by computing the integrals appearing in the second variation in closed form. The resulting equations constitute a generalized eigenvalue problem that depends on the aspect ratio of the buckle pattern λ/b (see fig. 1) and the nondimensional parameters and nondimensional stress resultants defined herein. The smallest eigenvalue of the problem corresponds to buckling and is found by specifying a value of λ/b and by solving the corresponding generalized eigenvalue problem for its smallest eigenvalue. This process is repeated for successive values of λ/b until the overall smallest eigenvalue is found.

Results obtained by using the analysis described herein for uniform compression, uniform shear, pure in-plane bending (given by $\varepsilon_0 = -1$ and $\varepsilon_1 = 1$), and various combinations of these loads have been compared with other results for isotropic, orthotropic, and anisotropic plates obtained by using other analysis methods. These comparisons are discussed in references 1 and 2, and in every case the results described herein were found to be in good agreement with those obtained from other analyses. Results obtained for isotropic and specially orthotropic plates that are subjected to a general linear distribution of axial load across the plate width were also compared with results presented in references 7 through 13. In every case, the agreement was good.

Results and Discussion

Results are presented for clamped and simply supported plates loaded by a general linear distribution of axial load across the plate width, uniform shear load, and combinations of these loads. For convenience, plates loaded by a general linear distribution of axial load across the plate width are referred to herein as plates loaded by linearly varying edge loads. To obtain the various edge load distributions used herein, $\varepsilon_1 = 1$ was specified and ε_0 was varied. Sketches that show the linearly varying edge loads for several values of ε_0 are shown in figure 2. For loading cases that involve shear, a distinction is made between positive and negative shear loads whenever flexural anisotropy is present. A positive shear load corresponds to the shear load shown in figure 1. Although the analysis presented herein previously includes the means for applying combined loads by using subcritical loads, the combined loads considered in the present paper were applied as primary destabilizing loads.

Results are presented first for the familiar $[\pm\theta]_s$ angle-ply plates that are loaded by linearly varying edge loads or by combined loads. (Several results for corresponding $[\pm\theta]_s$ angle-ply plates that are subjected to uniform uniaxial compression, uniform shear, or pure in-plane bending loads have been presented in refs. 1 and 2.) These thin laminates are representative of spacecraft structural components and are made of a typical graphite-epoxy material with a longitudinal modulus $E_1 = 127.8$ GPa (18.5 $\times$ 10^6 psi), a transverse modulus $E_2 = 11.0$ GPa (1.6 $\times$ 10^6 psi), an in-plane shear modulus $G_{12} = 5.7$ GPa (0.832 $\times$ 10^6 psi), a major Poisson's ratio $\nu_{12} = 0.35$, and a nominal ply thickness of 0.127 mm (0.005 in.). Generic results are presented next, in terms of the nondimensional parameters described herein, for ranges of parameters that are applicable to a broad class of laminate constructions. The term "generic" is used herein to emphasize that these buckling results are very general because they are presented in a form that is independent of the details of laminate construction; i.e., stacking sequence and ply materials. The ranges of the nondimensional parameters used herein are given by $0.1 \leq \beta \leq 3.0$, $0 \leq \gamma \leq 0.6$, and $0 \leq \delta \leq 0.6$. The results presented in references 1 and 2 indicate that $\gamma = \delta = 0.6$ corresponds to a highly anisotropic plate. For isotropic plates, $\beta = 1$ and $\gamma = \delta = 0$. Moreover, for symmetrically laminated plates without flexural anisotropy, $\gamma = \delta = 0$. (These plates are referred to herein as specially orthotropic plates.) Values of these nondimensional parameters that correspond to several practical laminates (and several material systems) are given in references 1 and 2.

To simplify the presentation of the fundamental generic behavioral trends, results are presented herein only for plates in which γ and δ have equal values (e.g., $[\pm 45]_s$ laminates). However, these behavioral trends are expected to be applicable to laminates with nearly equal values of γ and δ such as a $[+35/-15]_s$ laminate made of the typical graphite-epoxy material described herein. For this laminate, $\beta = 1.95$, $\gamma = 0.52$, and $\delta = 0.51$. Furthermore, results showing the effects of α_∞, or equivalently $(D_{11}/D_{22})^{1/4}$, on the buckling coefficients are not presented. References 1 and 2 have shown that variations in this parameter affect the critical value of the buckle aspect ratio λ/b but not the buckling coefficient (i.e., the buckling coefficient remains constant) of plates that are subjected to uniform tension or compression loads, uniform shear loads, and pure in-plane bending loads. This trend was found in the present study to be valid also for the plates loaded by linearly varying edge loads and uniform shear loads considered herein. For clarity, the shear and in-plane bending buckling coefficients, defined by equations (20) and (21), respectively, are expressed as $K_s\big|_{\gamma=\delta=0}$ and $K_b\big|_{\gamma=\delta=0}$ when the generic results are

described for plates in which flexural anisotropy is neglected in the buckling calculations.

Plates Loaded by Linearly Varying Edge Loads or Shear

Results are presented in figures 2 and 3 for simply supported and clamped $[\pm45]_s$ plates, respectively, that are subjected to linearly varying edge loads that correspond to values of $\varepsilon_0 = -2, -1.5, -1, -0.5, 0, 0.5,$ and 1. In these figures, the minimum value of the loading parameter $\bar{p}$, found by solving the generalized eigenvalue problem for a given value of λ/b, is shown by the solid lines for values of $0 \leq \lambda/b \leq 2$ (flexural anisotropy is included in the analysis). The overall minimum value of the loading parameter for each curve is indicated by an unfilled circle, and these minimum values of the loading parameter correspond to the value of the buckling coefficient for each curve. The corresponding values of λ/b are the critical values of the buckle aspect ratio.

The results presented in figures 2 and 3 show the effect of the load distribution shape and boundary conditions on the buckling coefficient and the corresponding critical value of λ/b. As the amount of tension load in the load distribution increases (ε_0 decreases), the buckling coefficient increases substantially, and the critical value of λ/b decreases. Moreover, the results show that the clamped plates exhibit larger buckling coefficients and smaller critical values of λ/b than corresponding simply supported plates. As the amount of tension load in a linearly varying edge load distribution increases, the amount of the plate width that is in compression decreases. As a result, the buckles appearing in the plate are typically confined to the narrower compression region. The width d of this narrower compression region of a plate is obtained from the equation that defines the corresponding neutral axis of the in-plane bending load component (defined by $N_x = 0$); that is, $d = b/(1 - \varepsilon_0)$ where $\varepsilon_0 < 0$. For plates with large negative values of ε_0, the critical value of λ/b may be much less than a value of 1. For these cases, a more accurate expression of the critical buckle aspect ratio is given by λ/d.

Results that indicate the effect of the edge load distribution shape on the buckling coefficients for simply supported and clamped $[\pm\theta]_s$ plates with $\theta = 0°, 30°, 45°, 60°,$ and $90°$ (see fig. 1) are shown in figure 4. The solid and dashed lines correspond to buckling coefficients for clamped and simply supported plates, respectively, in which the flexural anisotropy is neglected in the analysis. These results show that the clamped plates always have higher buckling coefficients than the simply supported plates and that the buckling coefficients for the clamped plates are more sensitive to variations in the load

distribution parameter ε_0 (indicated by the slope of the curves). The results also show very large increases in buckling coefficient as the amount of tension in the edge load distribution increases (ε_0 decreases) for all values of θ. For a given value of ε_0, the largest buckling coefficient is exhibited by the plates with $\theta = 45°$, followed by the plates with $\theta = 30°$ and $60°$, and then by the plates with $\theta = 0°$ and $90°$. Moreover, the results indicate that the plates with $\theta = 30°$ and $60°$ have the same buckling coefficients as do the plates with $\theta = 0°$ and $90°$.

The importance of neglecting the anisotropy in the calculation of the buckling coefficients given in figure 4 for $[\pm\theta]_s$ plates is indicated in figure 5. In figure 5, the ratio of the anisotropic-plate buckling coefficient K_b to the corresponding specially orthotropic-plate buckling coefficient $K_b\big|_{\gamma=\delta=0}$ is given as a function of the load distribution parameter ε_0 and the fiber angle θ. The solid and dashed lines shown in the figure correspond to results for clamped and simply supported plates, respectively. The results indicate that the simply supported plates generally exhibit larger reductions in the buckling coefficient ratio because of anisotropy and that the simply supported plates are more sensitive to the load distribution parameter ε_0 than are the clamped plates. In particular, the results predict that the simply supported plates are only slightly sensitive to variations in ε_0 and that the clamped plates exhibit practically no sensitivity to variations in ε_0. The largest reductions in the buckling coefficient ratio are predicted for the plates with $\theta = 45°$, followed by the plates with $\theta = 60°$ and $\theta = 30°$, respectively. The simply supported plates with $\theta = 45°$ and with $\varepsilon_0 = -2$ and $\varepsilon_0 = 1$ (uniform compression) have values of approximately 0.76 and 0.74, respectively, for the buckling coefficient ratio.

Generic effects of plate orthotropy. Generic buckling results for specially orthotropic ($\gamma = \delta = 0$) simply supported and clamped plates that are subjected to linearly varying edge loads are presented in figures 6 through 10. The solid and dashed lines in the figures correspond to results for clamped and simply supported plates, respectively. The results presented in figure 6 show the buckling coefficient as a function of the orthotropy parameter β for selected values of the load distribution parameter $\varepsilon_0 = -2, -1.5,$ and -1. Similar results are presented in figure 7 for values of $\varepsilon_0 = -0.5, 0, 0.5,$ and 1. The results presented in figures 8 through 10 show the buckling coefficient as a function of the load distribution parameter ε_0 for discrete values of the orthotropy parameter $\beta = 0.5, 1, 1.5, 2, 2.5,$ and 3. In figures 8 through 10, results are presented for $-2 \leq \varepsilon_0 \leq -1$, $-1 \leq \varepsilon_0 \leq 0$, and $0 \leq \varepsilon_0 \leq 1$, respectively, because of the large variation in the buckling coefficient with ε_0.

The generic results presented in figures 6 through 10 show that the buckling coefficient increases substantially as the orthotropy parameter β increases. In contrast, the buckling coefficient decreases substantially as the load distribution parameter ε_0 increases and the amount of compression in the load distribution increases. In addition, the results presented in figures 6 and 7 indicate that the clamped plates are more sensitive to variations in the orthotropy parameter β (indicated by the slope of the curves) than the simply supported plates for the full range of load distribution parameters considered. Moreover, the results presented in figures 8 through 10 indicate that for a given value of β, the clamped plates are typically more sensitive to variations in the load distribution parameter ε_0 than are the simply supported plates.

Some generic buckling results for specially orthotropic simply supported and clamped shear-loaded plates that have been presented in references 1, 2, and 5 are presented in figure 11 for completeness of the present study and for convenience. The solid and dashed lines in the figure show the buckling coefficient as a function of the orthotropy parameter β for clamped and simply supported plates, respectively. The results indicate that the shear buckling coefficient increases substantially as the orthotropy parameter β increases and that the clamped plates are typically more sensitive to variations in β than are the simply supported plates. This trend for the shear-loaded plates is the same as the corresponding trend predicted for the plates that are loaded by linearly varying edge loads.

Generic effects of plate anisotropy. Results are presented in figures 12 through 16 for simply supported and clamped plates that are subjected to linearly varying edge loads. In figures 12 through 16, the ratio of the anisotropic-plate buckling coefficient K_b to the corresponding specially orthotropic-plate buckling coefficient $K_b\big|_{\gamma=\delta=0}$ (see figs. 6 through 10) is given for equal values of the anisotropy parameters ($\gamma = \delta$) ranging from 0.1 to 0.6. In figures 12 and 13, the generic effects of plate anisotropy on the buckling coefficient ratio are given for simply supported and clamped plates, respectively, as a function of the orthotropy parameter β. For each value of $\gamma = \delta$ given in figures 12 and 13, two curves are presented. The solid and dashed lines correspond to values of the load distribution parameter $\varepsilon_0 = 1$ (uniform compression) and $\varepsilon_0 = -2$ (the maximum amount of tension in the load distributions considered herein), respectively. In figures 14 through 16, the buckling coefficient ratio is given as a function of the load distribution parameter ε_0 for discrete values of the orthotropy parameter $\beta = 3, 1.5,$ and 0.5, respectively. The solid and dashed lines in

figures 14 through 16 correspond to results for clamped and simply supported plates, respectively.

Figures 12 through 16 show that the anisotropic-plate buckling coefficient is always less than the corresponding orthotropic-plate buckling coefficient for all values of parameters considered. In addition, these results predict that the effects of neglecting anisotropy are typically more pronounced for the simply supported plates than for the clamped plates, but only by a small amount. Moreover, for the full range of anisotropy considered, figures 12 and 13 show a trend of monotonic increase in the buckling coefficient ratio as the orthotropy parameter β increases. The results in figures 12 through 16 also predict that the effects of neglecting plate flexural anisotropy in the buckling analysis of simply supported plates become slightly less pronounced as the load distribution parameter ε_0 decreases and the amount of tension in the edge load distribution increases. Moreover, this effect is practically negligible in the corresponding clamped plates. This behavioral trend, in which the importance of anisotropy is reduced as the amount of tension in the edge load distribution increases, is similar to a behavioral trend given in reference 5. There, the importance of anisotropy on the buckling load of a plate that is subjected to destabilizing uniform axial compression is shown to be reduced as the amount of subcritical transverse tension load N_{y2} that is applied to the plate is increased. However, for this case, the clamped plates exhibit more sensitivity to the transverse tension load than do the simply supported plates.

Results that show the importance of flexural anisotropy on the buckling behavior of shear-loaded simply supported and clamped plates have been presented in reference 1 and are presented in figure 17 in a different form for convenience. In this figure, the ratio of the anisotropic-plate buckling coefficient K_s to the corresponding specially orthotropic-plate buckling coefficient $K_s\big|_{\gamma=\delta=0}$ (see fig. 11) is given as a function of the orthotropy parameter β for equal values of the anisotropy parameters ($\gamma = \delta$) ranging from 0.2 to 0.6. Two groups of curves that correspond to positive and negative shear loads are shown in the figure. For each value of $\gamma = \delta$ given in figure 17, two curves are presented in each group. The solid and dashed lines correspond to results for clamped and simply supported plates, respectively.

The results presented in figure 17 for simply supported and clamped plates that are subjected to positive shear loads indicate that the anisotropic-plate buckling coefficient is always less than the corresponding orthotropic-plate buckling coefficient. However, this trend is reversed for negative shear loads. The results in figure 17 also show that the effects of neglecting plate

7

anisotropy become smaller as the orthotropy parameter β increases and the anisotropy parameters γ and δ decrease. Furthermore, these results show that the effects of neglecting plate anisotropy are only slightly more pronounced for simply supported plates than for clamped plates. Comparing the results presented in figures 12, 13, and 17 indicates that the reductions in buckling coefficient caused by neglecting anisotropy are, for the most part, more pronounced for the shear-loaded plates than for the plates that are subjected to linearly varying edge loads.

Plates Loaded by Shear and Linearly Varying Edge Loads

Buckling interaction curves obtained by neglecting the plate anisotropy in the buckling calculations for simply supported $[\pm 45]_s$ plates that are subjected to uniform shear and linearly varying edge loads are presented in figure 18. Negative values of K_b indicated on the figure correspond to results in which the sign of N_{b1} is reversed, and negative values of K_s correspond to negative shear loadings. Several curves that indicate the stability boundaries corresponding to values of the load distribution parameter $\varepsilon_0 = -2, -1.5, -1, -0.5, 0, 0.5,$ and 1 are presented in figure 18. Each curve shown in the figure is symmetric about the line $K_s = 0$, and the curve for $\varepsilon_0 = -1$ (pure in-plane bending) is also symmetric about the line $K_b = 0$. In addition, all the curves pass through the same two points on the line $K_b = 0$; i.e., the points that correspond to positive and negative shear buckling.

The curves shown in figure 18 for values of $\varepsilon_0 = 0$, 0.5, and 1 are open, parabola-like curves that extend indefinitely in the negative K_b-direction. For these combined loadings, shear loads that are greater in magnitude than the shear buckling load can be sustained only when the linearly varying edge loads are tensile loads. In contrast, specially orthotropic plates that are subjected to pure in-plane bending ($\varepsilon_0 = -1$) can never sustain shear loads that are greater in magnitude than the shear buckling load. However, the curves shown in figure 18 for $\varepsilon_0 = -2, -1.5,$ and -0.5 are significantly different from the conventional buckling interaction curves found in the literature and shown in figure 18 for plates that are subjected to uniform shear and uniform axial compression ($\varepsilon_0 = 1$) or pure in-plane bending loads. Specifically, the results predict that shear loads that are larger in magnitude than the shear buckling load can be supported by an unbuckled plate when a tension-dominated linearly varying edge load distribution is applied to the plate first. It is important to observe that the loading with $\varepsilon_0 = -0.5$ is tension dominated for negative values of K_b but not for positive values. In general, when trying to determine whether a linearly varying edge load is tension dominated, both positive and negative values of K_b should be

considered. The ability to carry shear loads greater in magnitude than the positive and negative shear buckling loads is attributed to the fact that the stabilizing effect of the tension part of the linearly varying edge load is greater than the destabilizing effect of the compression part.

Additional buckling interaction curves that correspond to the curves shown in figure 18 are presented in figure 19 for simply supported $[\pm 45]_s$ plates that are subjected to shear and linearly varying edge loads. The curves shown in figure 19 include the effects of flexural anisotropy which are manifested by skewing and translation of the curves presented in figure 18 in the K_b-K_s plane. Thus, the results indicate that for a given value of K_b, the anisotropic plates can carry a negative shear load that is much greater in magnitude than the corresponding positive shear load. Moreover, the results predict that the anisotropic plates with a tension-dominated linearly varying edge load distribution (i.e., $\varepsilon_0 = -2, -1.5,$ and -0.5) can also support shear loads (positive or negative) that are larger in magnitude than the shear buckling load and that this effect is much more pronounced for plates that are loaded in negative shear. This greater negative-shear load capacity for the plates is attributed to the greater shear buckling resistance of these plates under negative shear loads. That is, flexurally anisotropic plates generally exhibit two unequal plate bending stiffnesses along the directions of the diagonal compression and tension generated by the shear load. For a negative shear load, the higher plate bending stiffness acts in the direction of the diagonal compression generated by the load.

The importance of neglecting anisotropy in the calculation of buckling interaction curves for simply supported $[\pm\theta]_s$ plates that are loaded by shear and a tension-dominated linearly varying edge load distribution ($\varepsilon_0 = -2$) is indicated in figure 20. Curves are shown in this figure for values of $\theta = 30°, 45°,$ and $60°$. The solid and dashed lines are buckling interaction curves in which the plate anisotropy is neglected (specially orthotropic) and included, respectively. Figure 20 indicates that the specially orthotropic plates with $\theta = 45°$ have larger (in magnitude) buckling coefficients than the corresponding plates with $\theta = 30°$ and $60°$. Moreover, the buckling interaction curves for the specially orthotropic plates with $\theta = 30°$ and $60°$ are identical. For the anisotropic plates, however, these two trends are not valid. That is, the buckling coefficients for the anisotropic plates with $\theta = 45°$ are not always larger in magnitude than the buckling coefficients for the corresponding plates with $\theta = 30°$ and $60°$. Moreover, the buckling interaction curves for the anisotropic plates with $\theta = 30°$ and $60°$ are different. The results also predict the capability of carrying shear loads that are greater in magnitude than the shear buckling loads (positive and negative) for

all the specially orthotropic and anisotropic plates considered.

Generic effects of plate orthotropy.

Generic buckling interaction curves for specially orthotropic ($\gamma = \delta = 0$) simply supported plates that have a value of $\beta = 3$ and that are subjected to shear and linearly varying edge loads are presented in figure 21. In particular, several curves that indicate the stability boundaries that correspond to values of the load distribution parameter $\varepsilon_0 = -2, -1.5, -1, -0.5, 0, 0.5$, and 1 are presented in the figure. The generic buckling interaction curves shown in figure 21 exhibit the same characteristics as the corresponding curves presented in figure 18 for the $[\pm 45]_s$ plates in which the effects of anisotropy are neglected. That is, each curve shown in the figure is symmetric about the line given by a zero value of $K_s\big|_{\gamma=\delta=0}$, and the curve for $\varepsilon_0 = -1$ (pure in-plane bending) is also symmetric about the line given by a zero value of $K_b\big|_{\gamma=\delta=0}$. In addition, all the curves pass through the same two points on the line given by a zero value of $K_b\big|_{\gamma=\delta=0}$, i.e., the points that correspond to positive and negative shear buckling. Like the results presented in figure 18 for the $[\pm 45]_s$ plates, the generic curves shown in figure 21 for values of $\varepsilon_0 = 0, 0.5$, and 1 are open, parabola-like curves that extend indefinitely in the negative $K_b\big|_{\gamma=\delta=0}$-direction. Thus, for these three loadings, shear loads that are greater in magnitude than the shear buckling load can be sustained only when the linearly varying edge loads are tensile loads. However, the plates that are subjected to pure in-plane bending ($\varepsilon_0 = -1$) can never sustain shear loads greater in magnitude than the shear buckling load. Furthermore, the generic results also predict an ability to carry shear loads that are larger in magnitude than the corresponding shear buckling load for plate loadings with $\varepsilon_0 = -2, -1.5$, and -0.5 (i.e., tension-dominated load distributions). This ability to carry shear loads greater in magnitude than the positive and negative shear buckling loads is again attributed to the fact that the stabilizing effect of the tension part of the linearly varying edge load is greater than the destabilizing effect of the compression part.

Generic buckling interaction design curves for specially orthotropic ($\gamma=\delta=0$) simply supported and clamped plates that are subjected to shear and linearly varying edge loads are presented in figures 22 through 28 for values of $\varepsilon_0 = -2, -1.5, -1, -0.5, 0, 0.5$, and 1, respectively. The solid lines and dashed lines in the figures correspond to results for clamped and simply supported plates, respectively, and curves are given for values of the

orthotropy parameter $\beta = 0.5, 1, 1.5, 2, 2.5$, and 3. Moreover, curves are shown for positive shear loading only. Results for negative shear loading are obtained by noting that buckling interaction curves for specially orthotropic plates that are loaded by shear are symmetric about the $K_b\big|_{\gamma=\delta=0}$-axis. Points on the curves correspond to constant values of the stiffness-weighted load ratio $\dfrac{N_{b1}}{N_{xy1}}\left(\dfrac{D_{22}}{D_{11}}\right)^{1/4}$, as illustrated in figure 29 by the line emanating from the origin of the plot. An important characteristic of all the buckling interaction curves presented in figures 22 through 28 is that, for a given stiffness-weighted load ratio, the magnitude of the buckling coefficients increases substantially as the orthotropy parameter β increases.

The results presented in figure 22 for the plates with $\varepsilon_0 = -2$ indicate that the maximum value of $K_s\big|_{\gamma=\delta=0}$ occurs within the range $2.86 \le \dfrac{N_{b1}}{N_{xy1}}\left(\dfrac{D_{22}}{D_{11}}\right)^{1/4} \le 4.44$ and $3.00 \le \dfrac{N_{b1}}{N_{xy1}}\left(\dfrac{D_{22}}{D_{11}}\right)^{1/4} \le 4.13$ for the simply supported and clamped plates, respectively, as the orthotropy parameter β increases from 0.5 to 3.0. Similarly, the results presented in figure 23 for the plates with $\varepsilon_0 = -1.5$ indicate that the maximum value of $K_s\big|_{\gamma=\delta=0}$ occurs within the range $2.64 \le \dfrac{N_{b1}}{N_{xy1}}\left(\dfrac{D_{22}}{D_{11}}\right)^{1/4} \le 3.97$ and $2.58 \le \dfrac{N_{b1}}{N_{xy1}}\left(\dfrac{D_{22}}{D_{11}}\right)^{1/4} \le 3.64$ for the simply supported and clamped plates, respectively. Moreover, the results presented in figure 25 for the plates with $\varepsilon_0 = -0.5$ indicate that the maximum value of $K_s\big|_{\gamma=\delta=0}$ occurs within the range $-8.88 \le \dfrac{N_{b1}}{N_{xy1}}\left(\dfrac{D_{22}}{D_{11}}\right)^{1/4} \le -5.72$ and $-8.31 \le \dfrac{N_{b1}}{N_{xy1}}\left(\dfrac{D_{22}}{D_{11}}\right)^{1/4} \le -6.00$ for the simply supported and clamped plates, respectively. Furthermore, the results presented in figure 24 for the plates with $\varepsilon_0 = -1$ indicate that the maximum value of $K_s\big|_{\gamma=\delta=0}$ occurs when $K_b\big|_{\gamma=\delta=0} = 0$.

The results presented in figures 24, 26, 27, and 28 for the plates with $\varepsilon_0 = -1, 0, 0.5$, and 1, respectively, indicate that the buckling interaction curves for the simply

supported plates generally have more curvature than the curves for the corresponding clamped plates. Thus, the simply supported plates are generally more sensitive to variations in the stiffness-weighted load ratio.

Generic effects of plate anisotropy. Generic buckling interaction curves for simply supported anisotropic plates with $\beta = 3$ and $\gamma = \delta = 0.6$ that are subjected to shear and linearly varying edge loads are presented in figure 30. More specifically, curves that indicate the stability boundaries for $\varepsilon_0 = -2, -1.5, -1, -0.5, 0, 0.5,$ and 1 are presented. The generic buckling interaction curves shown in figure 30 exhibit the same characteristics as the curves presented in figure 19 for the corresponding $[\pm45]_s$ anisotropic plates (these plates have $\beta = 2.28$ and $\gamma = \delta = 0.517$). That is, the effects of anisotropy are manifested by skewing and translation in the K_b-K_s plane of the curves for the corresponding specially orthotropic plates presented in figure 21. Thus, as was seen for the $[\pm45]_s$ anisotropic plates, the generic results for the anisotropic plates also predict that, for a given value of K_b, negative shear loads can be carried that are much greater in magnitude than the corresponding positive shear load. Moreover, the anisotropic plates with tension-dominated axial-edge load distributions ($\varepsilon_0 = -2, -1.5,$ and -0.5) can also support shear loads that are larger in magnitude than the shear buckling load. This effect is much more pronounced for plates that are loaded by negative shear. This difference in behavior exhibited by anisotropic and specially orthotropic plates loaded by negative and positive shear is attributed to directional dependence of the shear buckling resistance of anisotropic plates previously described herein.

Buckling interaction curves that show the generic effects of plate anisotropy are presented in figure 31 for simply supported and clamped plates with $\beta = 3$ that are subjected to shear and a linearly varying edge load corresponding to $\varepsilon_0 = -2$ (tension dominated). Several curves that indicate the stability boundaries for equal values of the anisotropy parameters ($\gamma = \delta$) ranging from 0 to 0.6 are shown in the figure. The solid and dashed lines in figure 31 correspond to results for clamped and simply supported plates, respectively. These results indicate that the curve corresponding to a specially orthotropic plate ($\gamma = \delta = 0$) becomes more skewed and is translated more in the negative K_s-direction as the values of the anisotropy parameters increase. These effects of anisotropy appear to be nearly the same for the clamped and simply supported plates.

The results presented in figure 31 also show that for some values of the stiffness-weighted load ratio $\dfrac{N_{b1}}{N_{xy1}}\left(\dfrac{D_{22}}{D_{11}}\right)^{1/4}$, the buckling interaction curves for plates

with $\gamma = \delta = 0$ and $\gamma = \delta \neq 0$ intersect. Thus, for these values of the stiffness-weighted load ratio, neglecting anisotropy has no effect on the critical value of the loading parameter $\tilde{p}_{cr}$ (see eqs. (18) through (21)). Moreover, the results indicate that as the stiffness-weighted load ratio varies, so does the importance of the plate anisotropy. An indication of the importance of plate anisotropy, with respect to the stiffness-weighted load ratio, is obtained by introducing the angle that the line emanating from the origin of the buckling interaction curve plot shown in figure 29 makes with the K_s-axis as an independent variable. This angle is referred to herein as the stiffness-weighted load ratio angle and is denoted by the symbol Ψ. Then, for a given stiffness-weighted load ratio (constant value of Ψ), the importance of anisotropy on the buckling coefficients is expressed by the ratio $\dfrac{\tilde{p}_{cr}}{\tilde{p}_{cr}\big|_{\gamma=\delta=0}}$ where

$$\frac{\tilde{p}_{cr}}{\tilde{p}_{cr}\big|_{\gamma=\delta=0}} = \frac{K_b}{K_b\big|_{\gamma=\delta=0}} = \frac{K_s}{K_s\big|_{\gamma=\delta=0}}.$$

Results are presented in figure 32 that show the importance of plate anisotropy on the buckling behavior of simply supported and clamped plates with $\beta = 3$ that are subjected to shear and a linearly varying edge load corresponding to $\varepsilon_0 = -2$. The results for the simply supported plates with $\gamma = \delta = 0.6$ correspond to those presented in figure 30. Curves that indicate the buckling coefficient ratio $\dfrac{\tilde{p}_{cr}}{\tilde{p}_{cr}\big|_{\gamma=\delta=0}}$ for equal values of the anisotropy parameters ($\gamma = \delta$) ranging from 0 to 0.6 are shown in figure 32 as a function of the stiffness-weighted load ratio angle Ψ. The solid and dashed lines in the figure correspond to results for clamped and simply supported plates, respectively. The results presented in the figure show a variation in the buckling coefficient ratio of approximately ±0.5, with the greatest variations occurring at values of $0° \leq \Psi \leq 70°$, $100° \leq \Psi \leq 200°$, and $290° \leq \Psi \leq 360°$. Moreover, the results indicate that the importance of plate anisotropy is only slightly more pronounced for the simply supported plates than for the clamped plates.

Concluding Remarks

A parametric study of the buckling behavior of infinitely long symmetrically laminated anisotropic plates that are subjected to linearly varying edge loads, uniform shear loads, or combinations of these loads has been presented. A special purpose nondimensional analysis that is well suited for parametric studies of clamped and simply

supported plates has been described, and its main features have been discussed. The results presented herein have focused on the effects of the shape of the linearly varying edge load distribution, plate flexural orthotropy, and plate flexural anisotropy on the buckling behavior. In addition, results have been presented that focus on the interaction of linearly varying edge loads and uniform shear loads with plate flexural anisotropy and orthotropy. In particular, results have been presented for $[\pm\theta]_s$ thin graphite-epoxy laminates that are representative of spacecraft structural components. Also, numerous generic buckling results have been presented that are applicable to a broad class of laminate constructions that show explicitly the effects of flexural orthotropy and flexural anisotropy on plate buckling behavior under these combined loads. These generic results can be used to extend the capability of existing design guides for plate buckling.

An important finding of the present study is that the buckling coefficients increase significantly as the orthotropy parameter $\beta = \dfrac{D_{12} + 2D_{66}}{(D_{11}D_{22})^{1/2}}$ increases or as the load distribution parameter ε_0 decreases (the loading distribution becomes tension dominated). In contrast, the buckling coefficients decrease significantly as the anisotropy parameters $\gamma = \dfrac{D_{16}}{(D_{11}^3 D_{22})^{1/4}}$ and $\delta = \dfrac{D_{26}}{(D_{11}D_{22}^3)^{1/4}}$ with equal values ($\gamma = \delta$) increase, for all linearly varying edge loads considered and for the plates that are subjected to positive shear loads. For negative shear loads, the trend is generally reversed. The effect of linearly varying edge load distribution shape (determined by ε_0) on the importance of plate anisotropy is generally small, with uniform compression-loaded plates exhibiting the largest reductions in buckling resistance. The results presented herein also show that the effects of plate anisotropy are slightly more pronounced for simply supported plates than for clamped plates when the plates are subjected to either linearly varying edge loads, uniform shear loads, or combinations of these loads. The most important finding of the present study is that specially orthotropic and flexurally anisotropic plates that are subjected to a tension-dominated axial edge load distribution (e.g., $\varepsilon_0 = -2, -1.5$, and -0.5) can support shear loads that are larger in magnitude than the shear buckling load. This ability to carry a shear load greater in magnitude than the corresponding shear buckling load is attributed to the fact that the stabilizing effect of the tension part of the linearly varying edge load is greater than the destabilizing effect of the compression

part. Moreover, this unusual behavior is much more pronounced for anisotropic plates than for specially orthotropic plates that are loaded in negative shear. This trend is reversed for plates that are loaded in positive shear. This difference in behavior exhibited by anisotropic plates and specially orthotropic plates loaded by negative shear and the trend reversal for positive shear loads is attributed to directional dependence of the shear buckling resistance of anisotropic plates.

NASA Langley Research Center
Hampton, VA 23681-2199
January 27, 1997

References

1. Nemeth, M. P.: Buckling Behavior of Long Symmetrically Laminated Plates Subjected to Combined Loadings. NASA TP-3195, 1992.

2. Nemeth, M. P.: Buckling of Symmetrically Laminated Plates With Compression, Shear, and In-Plane Bending. AIAA J., vol. 30, no. 12, Dec. 1992, pp. 2959–2965.

3. Zeggane, Madjid; and Sridharan, Srinivasan: Buckling Under Combined Loading of Shear Deformable Laminated Anisotropic Plates Using 'Infinite' Strips. Int. J. Numer. Methods in Eng., vol. 31, May 1991, pp. 1319–1331.

4. Zeggane, M.; and Sridharan, S.: Stability Analysis of Long Laminate Composite Plates Using Reissner-Mindlin 'Infinite' Strips. Comput. & Struct., vol. 40, no. 4, 1991, pp. 1033–1042.

5. Nemeth, Michael P.: Buckling Behavior of Long Anisotropic Plates Subjected to Combined Loads. NASA TP-3568, 1995.

6. Nemeth, Michael P.: Importance of Anisotropy of Buckling of Compression-Loaded Symmetric Composite Plates. AIAA J., vol. 24, no. 11, Nov. 1986, pp. 1831–1835.

7. Rockey, K. C.: Shear Buckling of Thin-Walled Sections. Thin-Walled Structures, A. H. Chilver, ed., John Wiley & Sons, Inc., 1967, pp. 261–262.

8. Oyibo, G. A.: The Use of Affine Transformations in the Analysis of Stability and Vibrations of Orthotropic Plates. Ph.D. Thesis, Rensselaer Polytechnic Inst., 1981.

9. Brunnelle, E. J.; and Oyibo, G. A.: Generic Buckling Curves for Specially Orthotropic Rectangular Plates. AIAA J., vol. 21, no. 8, Aug. 1983, pp. 1150–1156.

10. Timoshenko, Stephen P.; and Gere, James M.: Theory of Elastic Stability, Second ed. McGraw-Hill Book Co., 1961, pp. 373–379.

11. Bulson, P. S.: The Stability of Flat Plates. American Elsevier Publ. Co. Inc., 1969, pp. 63–77.

12. Bleich, Friedrich: Buckling Strength of Metal Structures. McGraw-Hill Co., Inc., 1952, pp. 399–413.

13. Galambos, Theodore V., ed.: Guide to Stability Design Criteria for Metal Structures. John Wiley & Sons, Inc., 1988, p. 103.
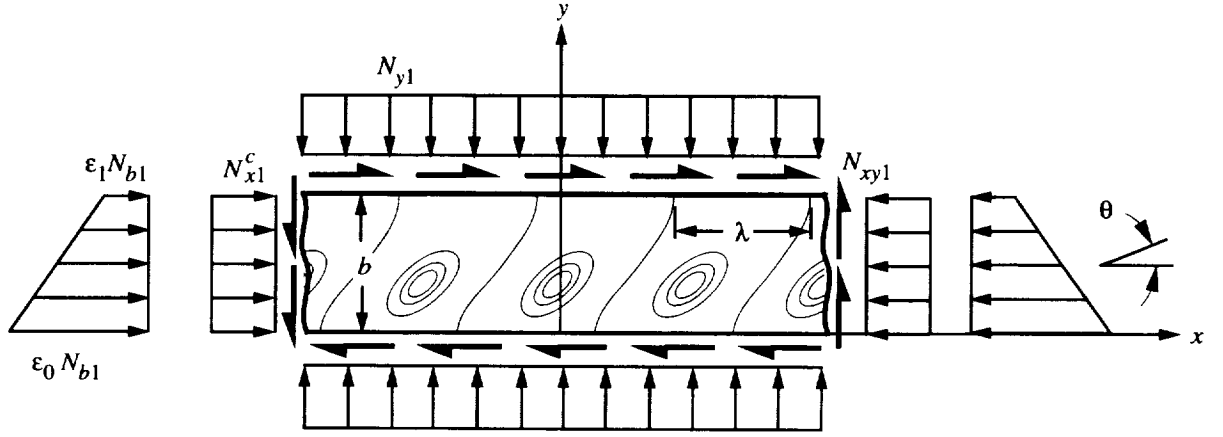
(a) Primary (destabilizing) loading system.
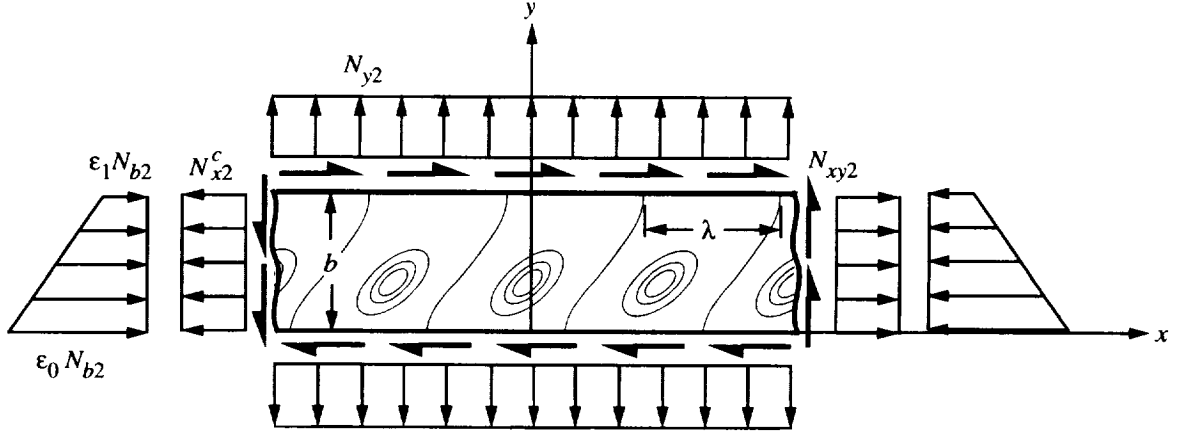
(b) Secondary (subcritical) loading system.

Figure 1. Loading systems and sign convention for positive-valued stress resultants ($\varepsilon_0 > \varepsilon_1 > 0$ shown above).
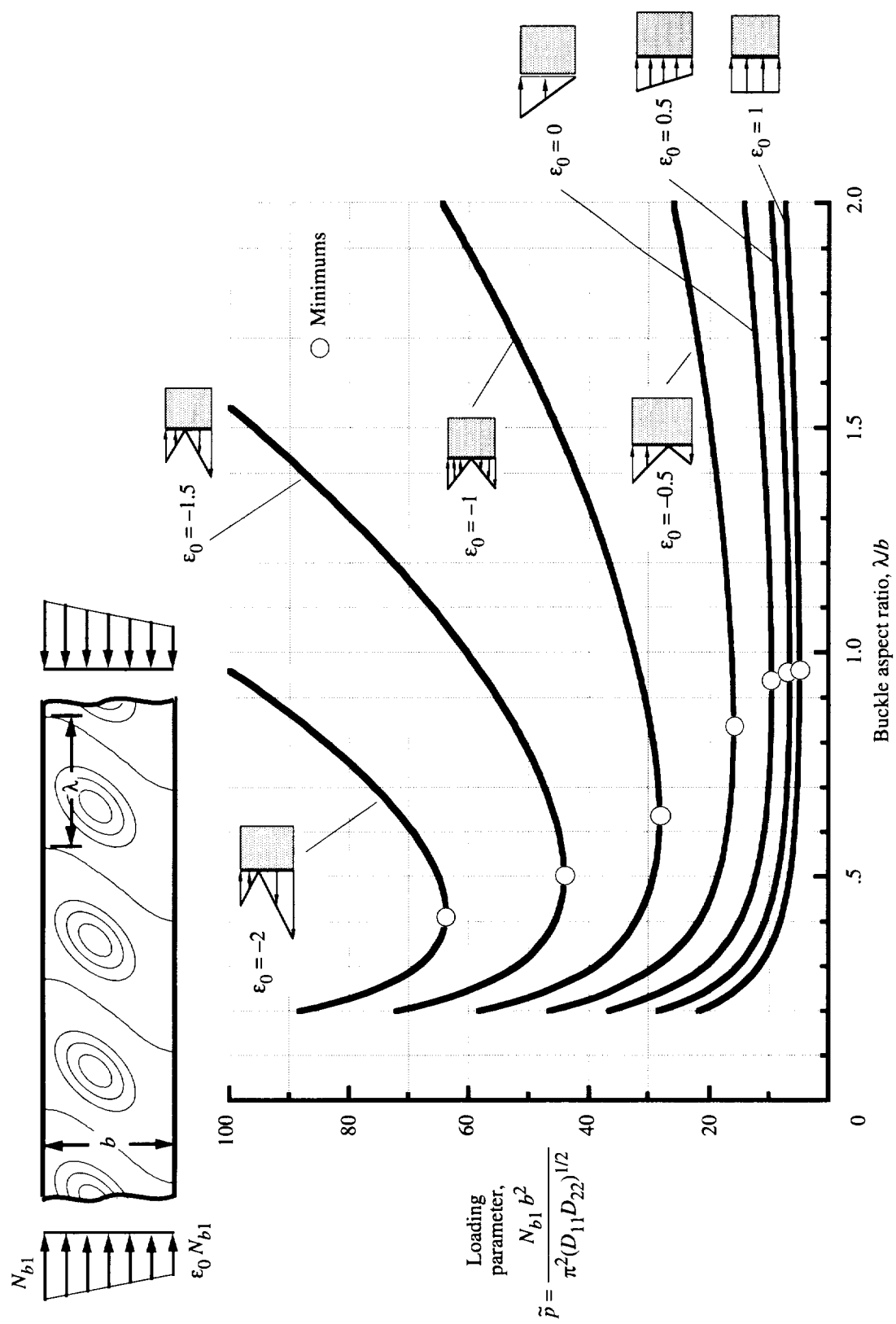
Figure 2. Buckling results for simply supported [±45]$_s$ plates subjected to linearly varying edge loads.
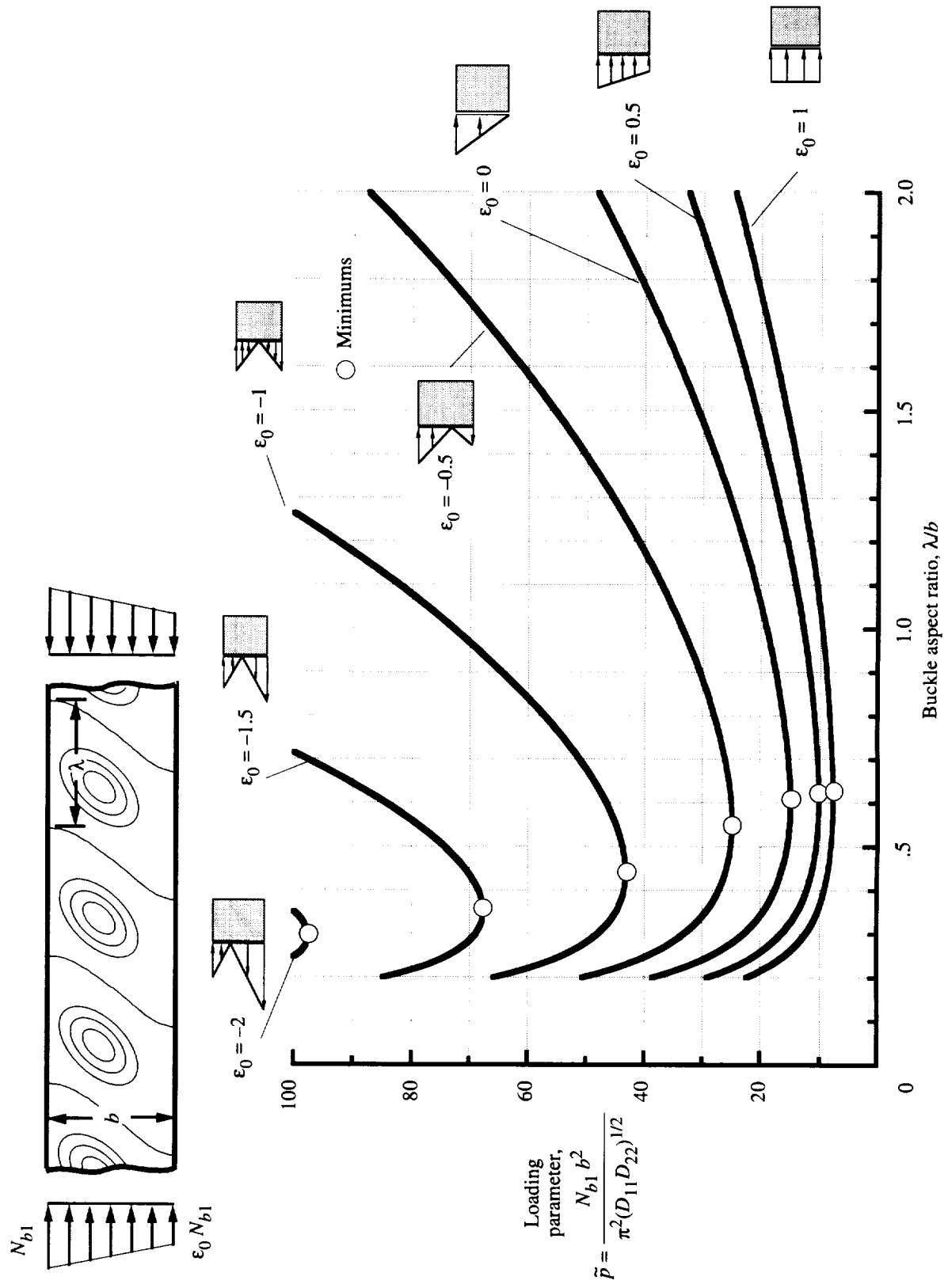
13

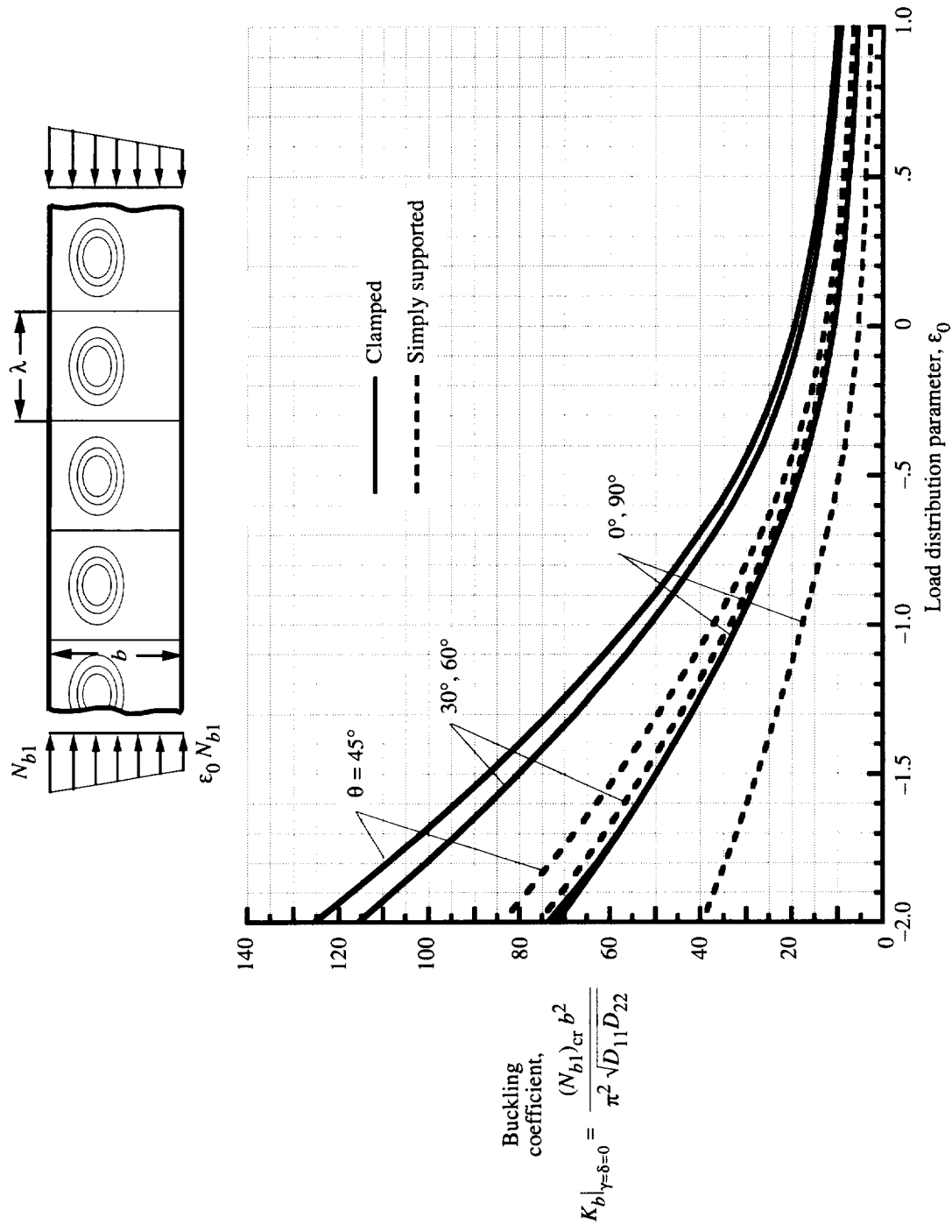Figure 3. Buckling results for clamped $[\pm 45]_s$ plates subjected to linearly varying edge loads.

14

Figure 4. Buckling coefficients for simply supported and clamped $[\pm\theta]_s$ plates subjected to linearly varying edge loads (anisotropy neglected in the analysis).
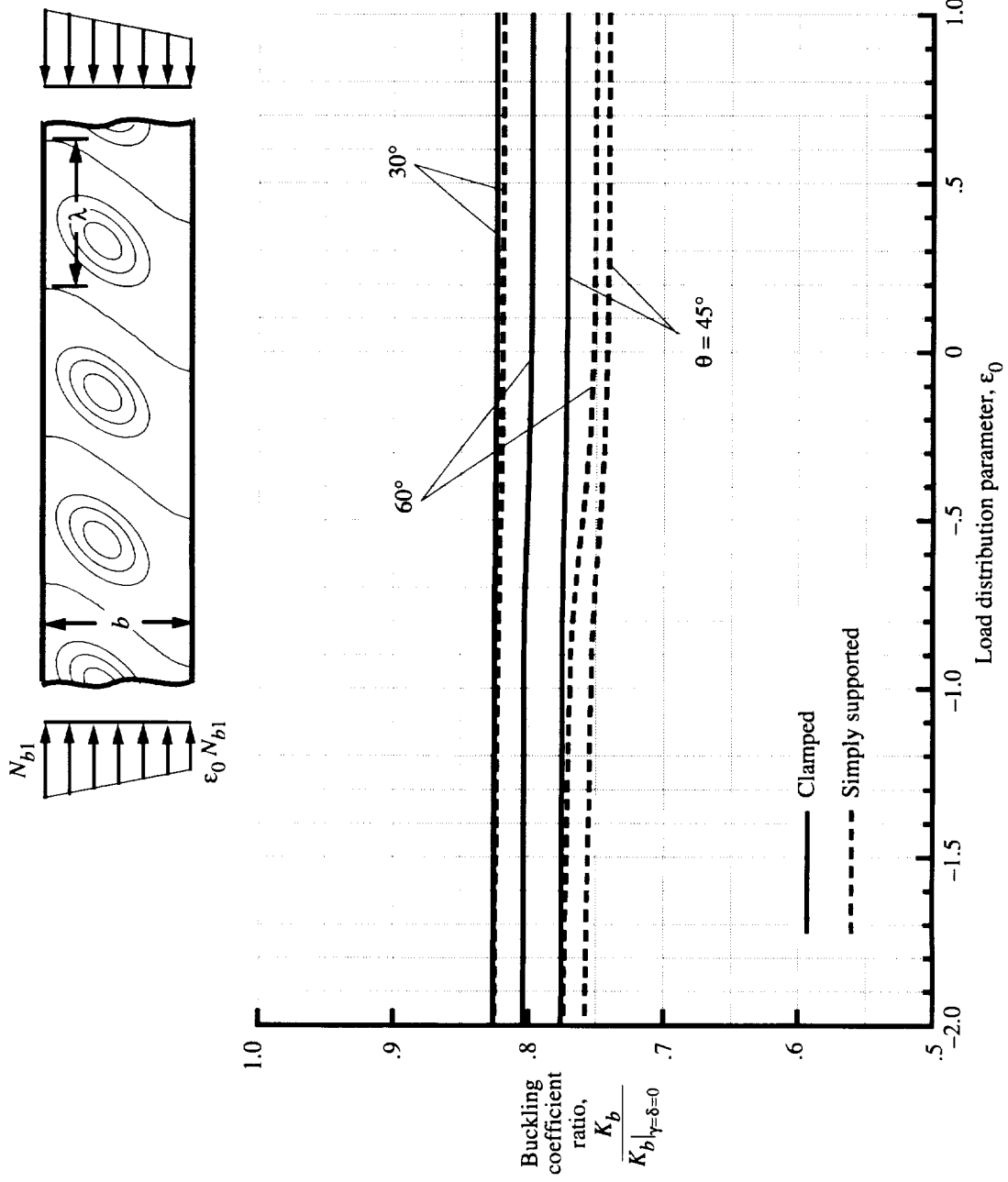
Figure 5. Ratio of anisotropic-to-orthotropic buckling coefficient for simply supported and clamped $[\pm\theta]_s$ plates subjected to linearly varying edge loads.
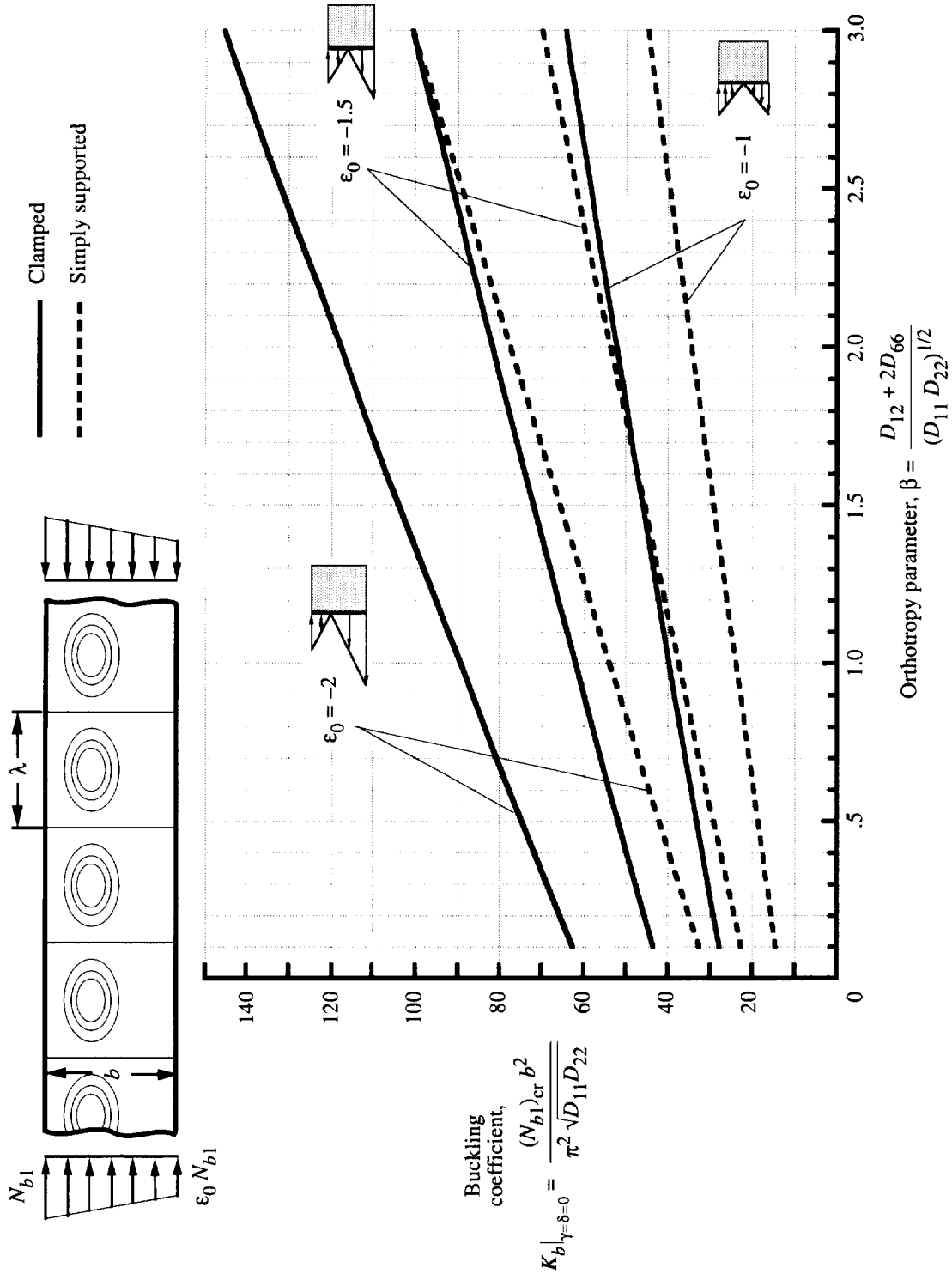
Figure 6. Effect of orthotropy parameter β on buckling coefficients for specially orthotropic plates ($\gamma = \delta = 0$) subjected to linearly varying edge loads ($\varepsilon_0 = -2$, -1.5, and -1).

17
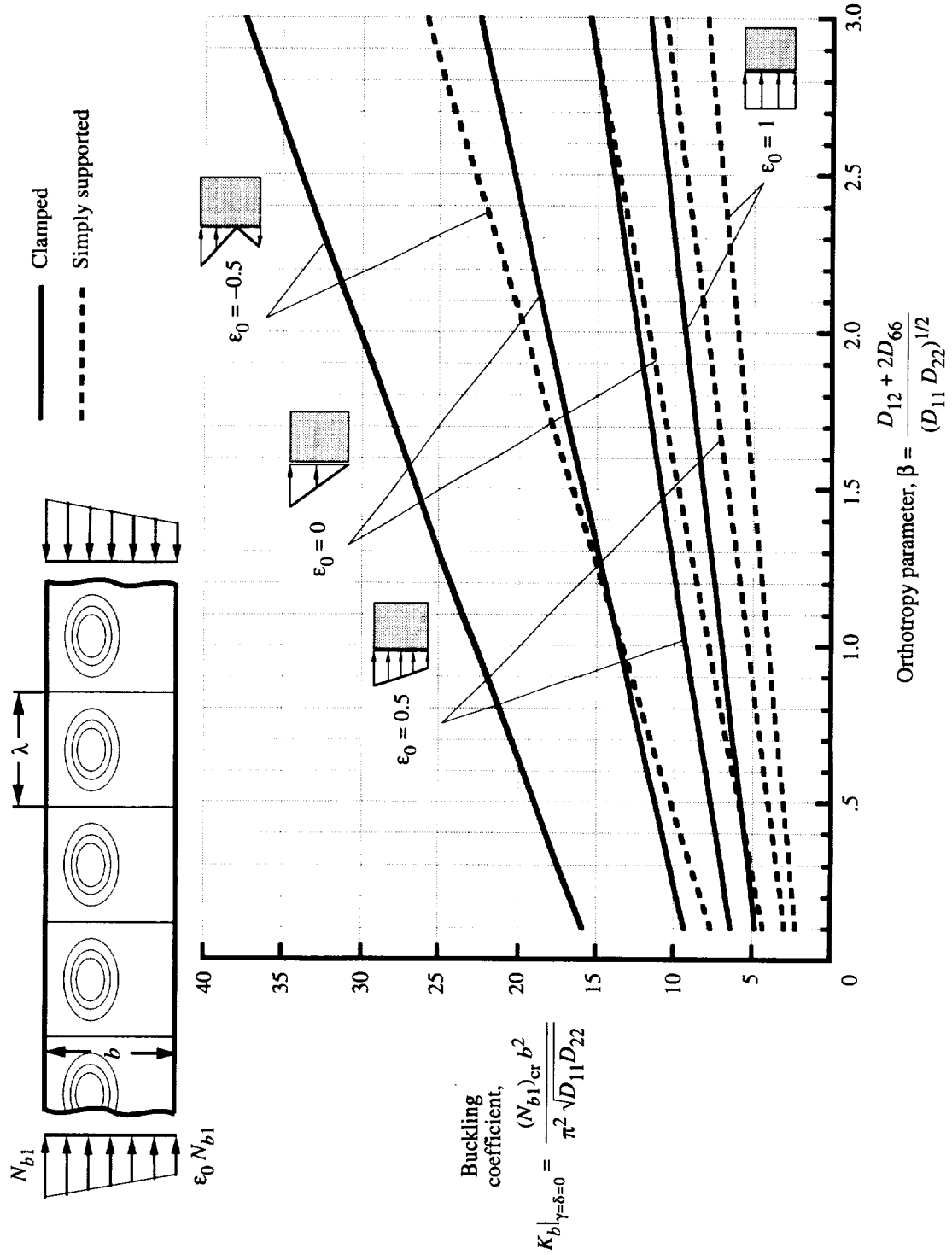
Figure 7. Effect of orthotropy parameter β on buckling coefficients for specially orthotropic plates ($\gamma = \delta = 0$) subjected to linearly varying edge loads ($\varepsilon_0 = -0.5$, 0, 0.5, and 1).
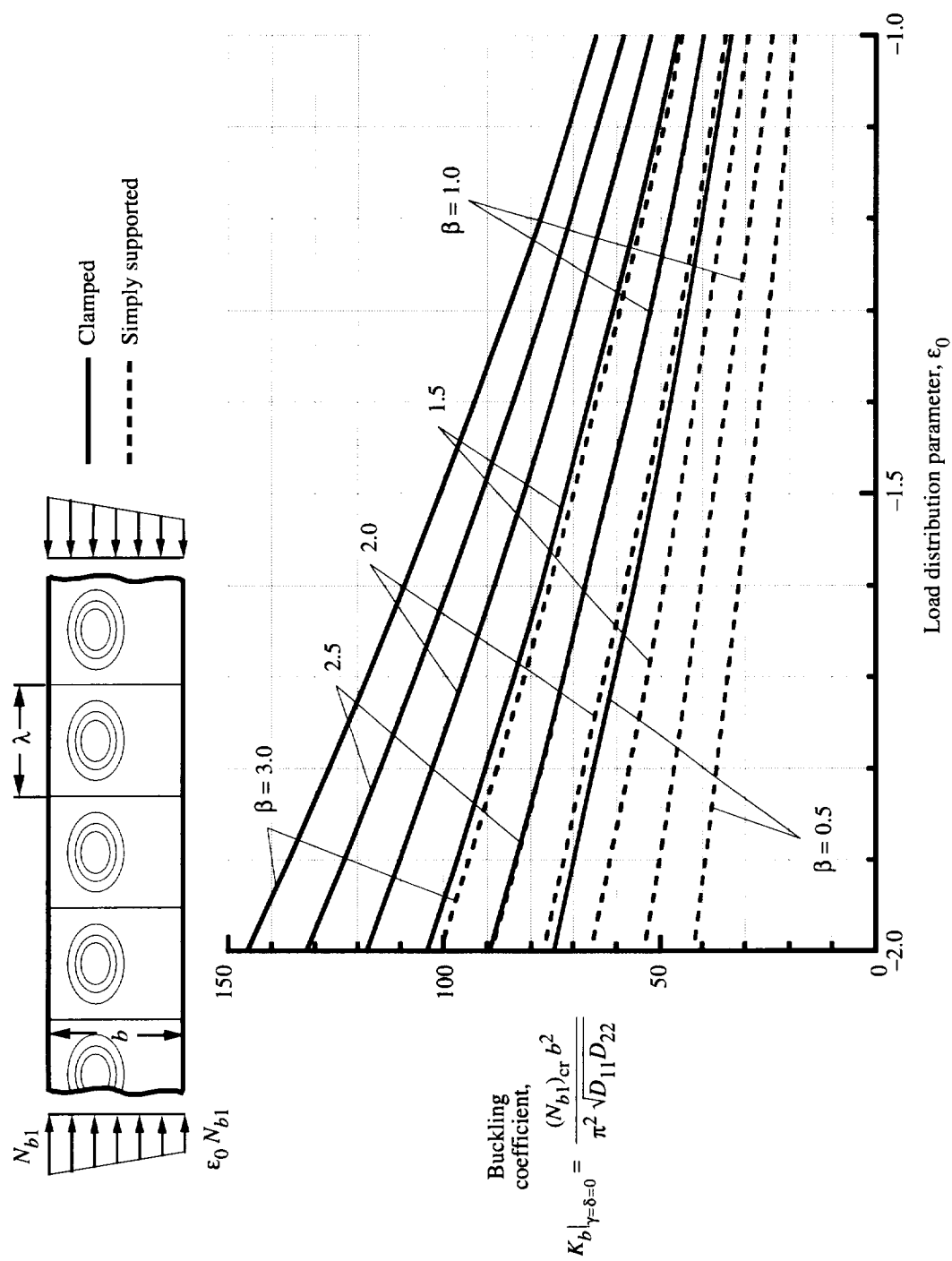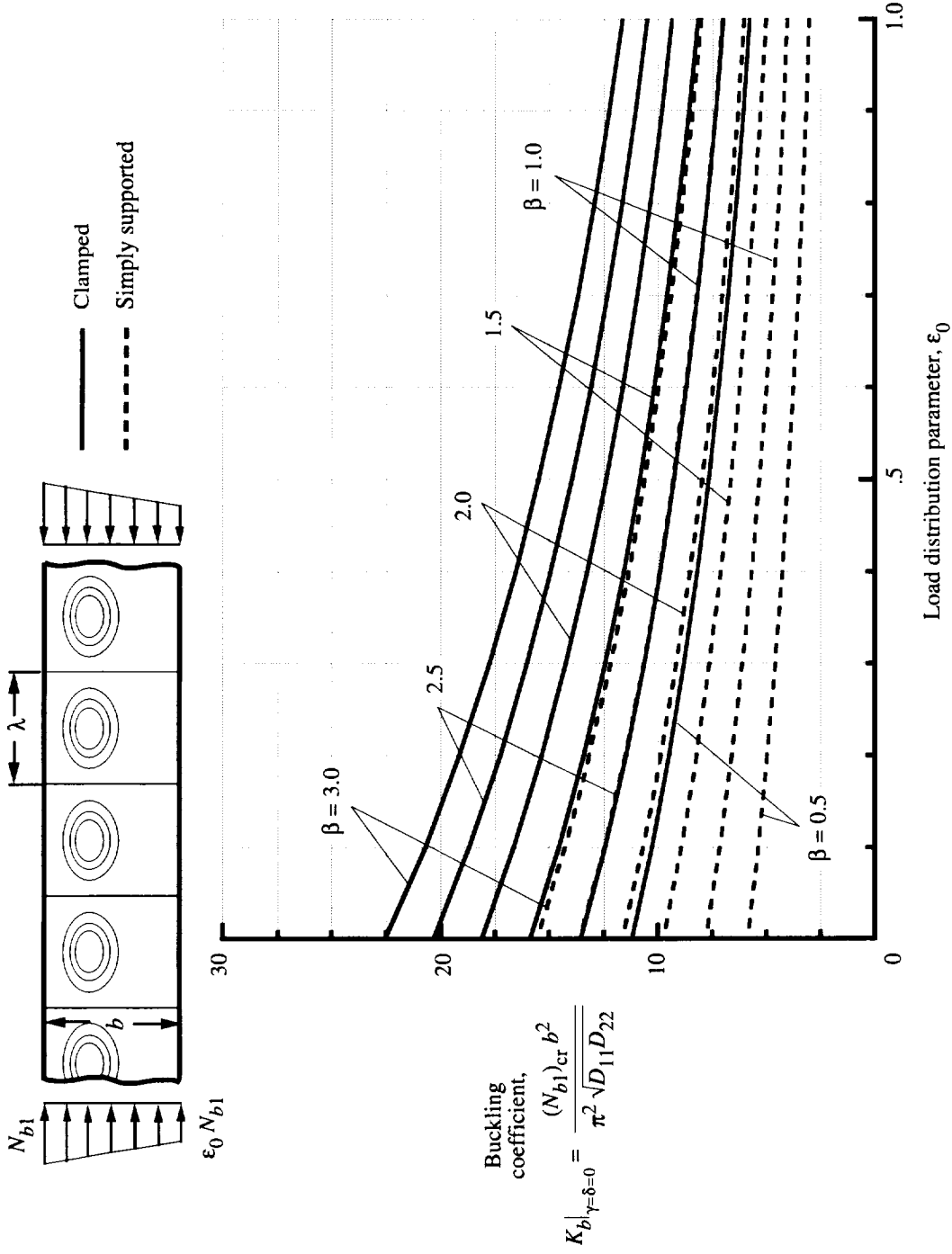
Figure 8. Effect of load distribution parameter ϵ_0 on buckling coefficients for specially orthotropic plates ($\gamma = \delta = 0$) subjected to linearly varying edge loads.
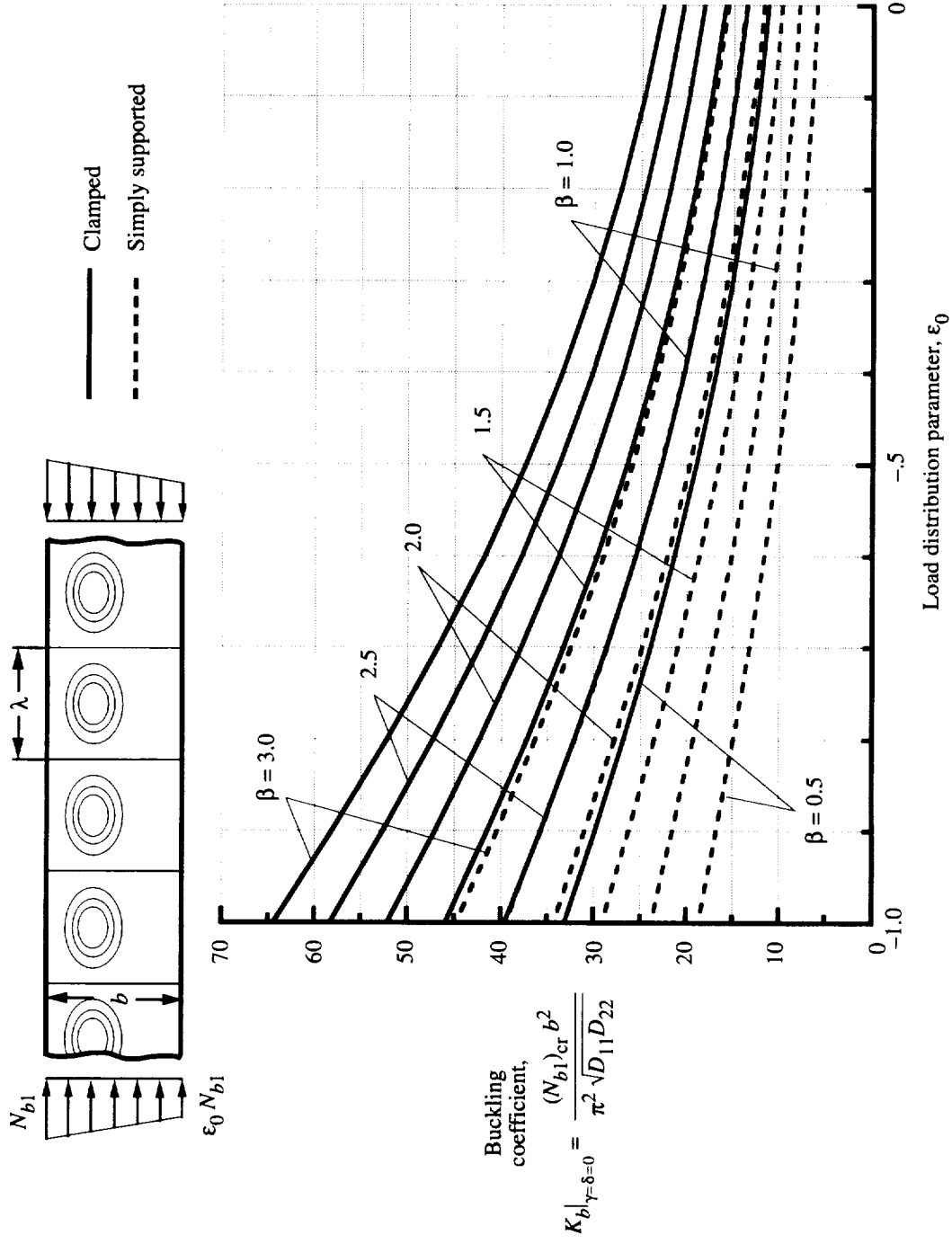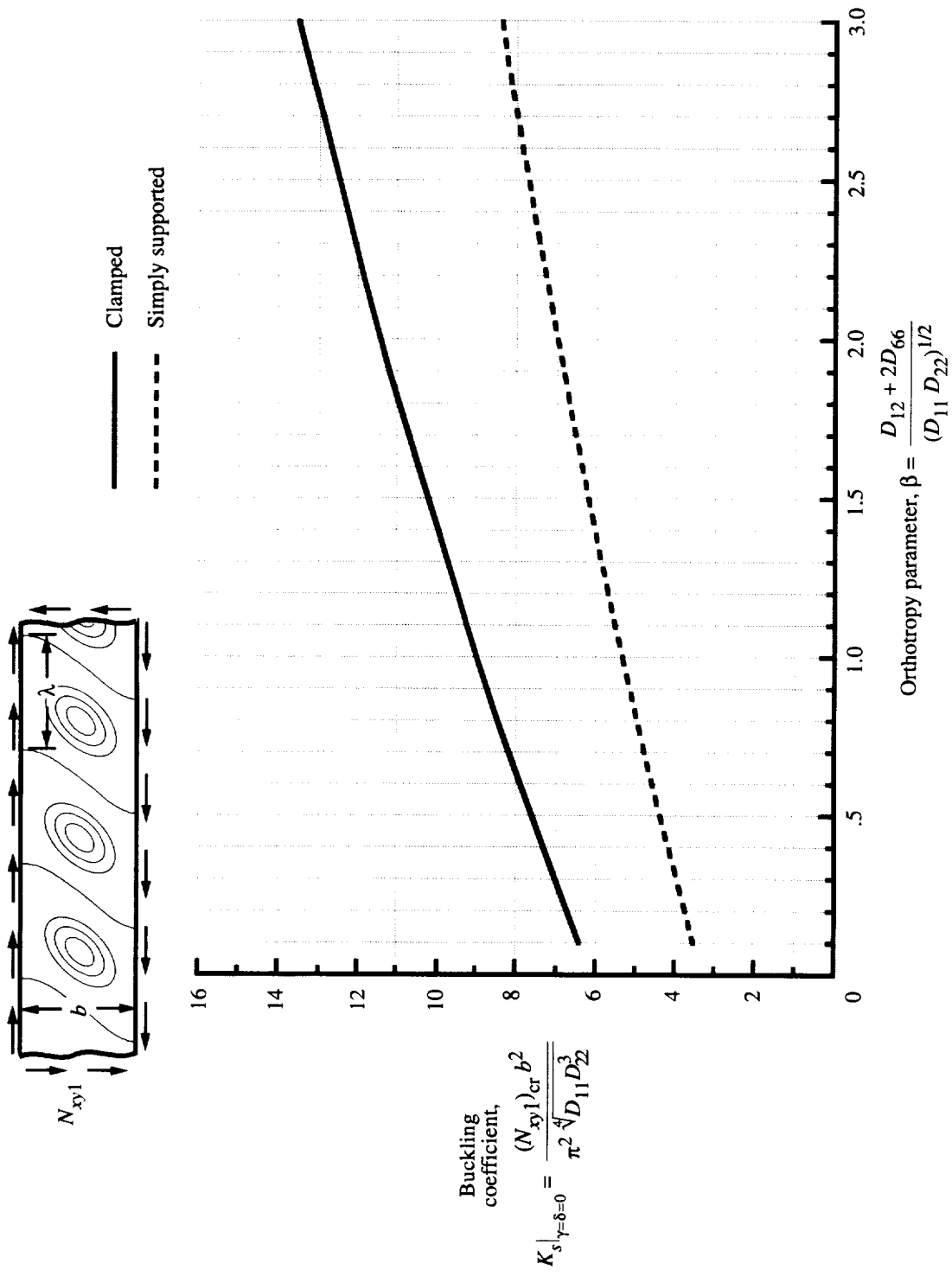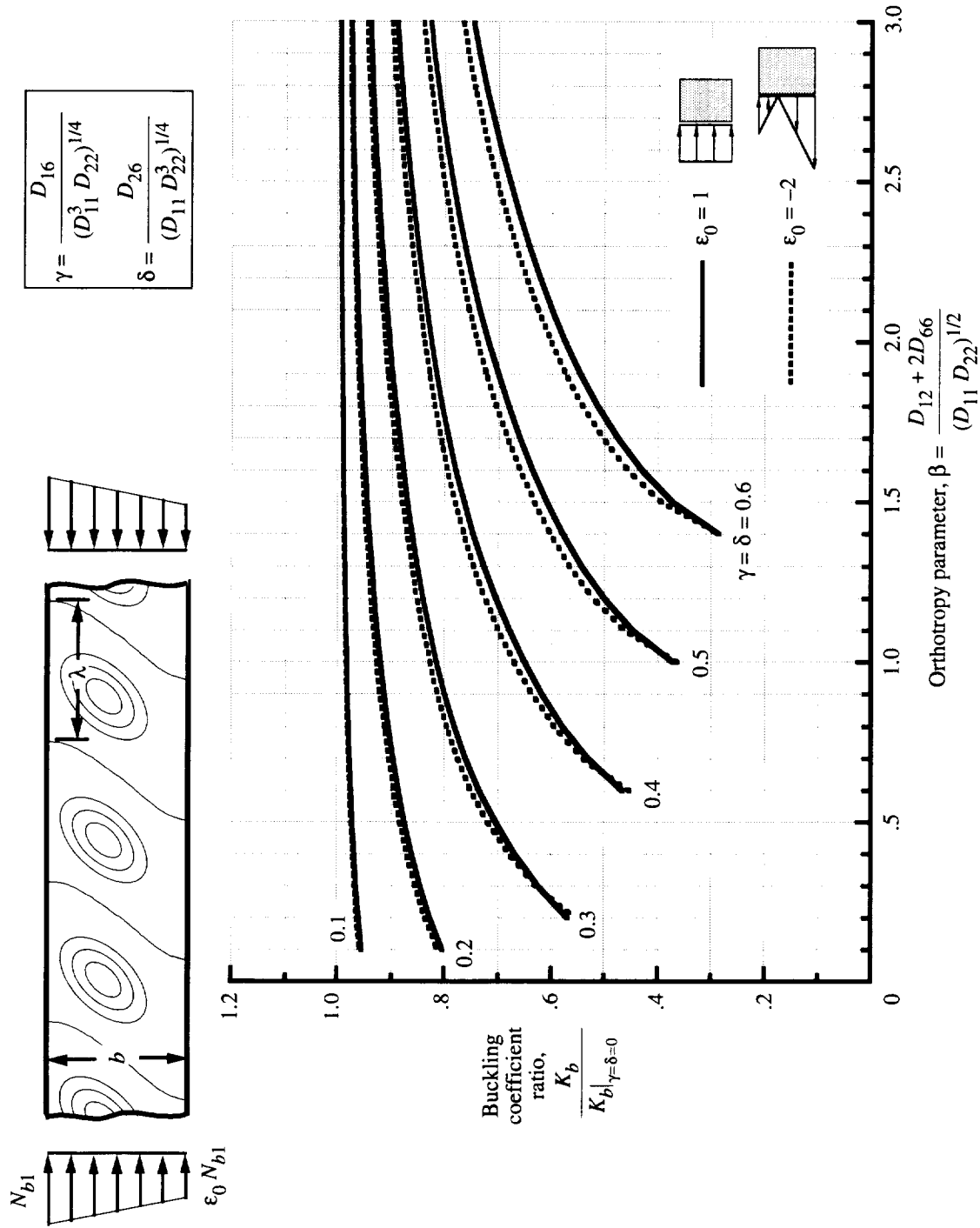
Figure 9. Effect of load distribution parameter ε_0 on buckling coefficients for specially orthotropic plates ($\gamma = \delta = 0$) subjected to linearly varying edge loads.

Figure 10. Effect of load distribution parameter ε_0 on buckling coefficients for specially orthotropic plates ($\gamma = \delta = 0$) subjected to linearly varying edge loads.

Buckling coefficient,

$$K_b\big|_{\gamma=\delta=0} = \frac{(N_{b1})_{cr} \, b^2}{\pi^2 \sqrt{D_{11}D_{22}}}$$

Figure 11. Effect of orthotropy parameter β on buckling coefficients for specially orthotropic plates ($\gamma = \delta = 0$) subjected to shear loads.

Figure 12. Effect of orthotropy parameter β and anisotropy parameters γ and δ on buckling coefficients for simply supported plates subjected to linearly varying edge loads.
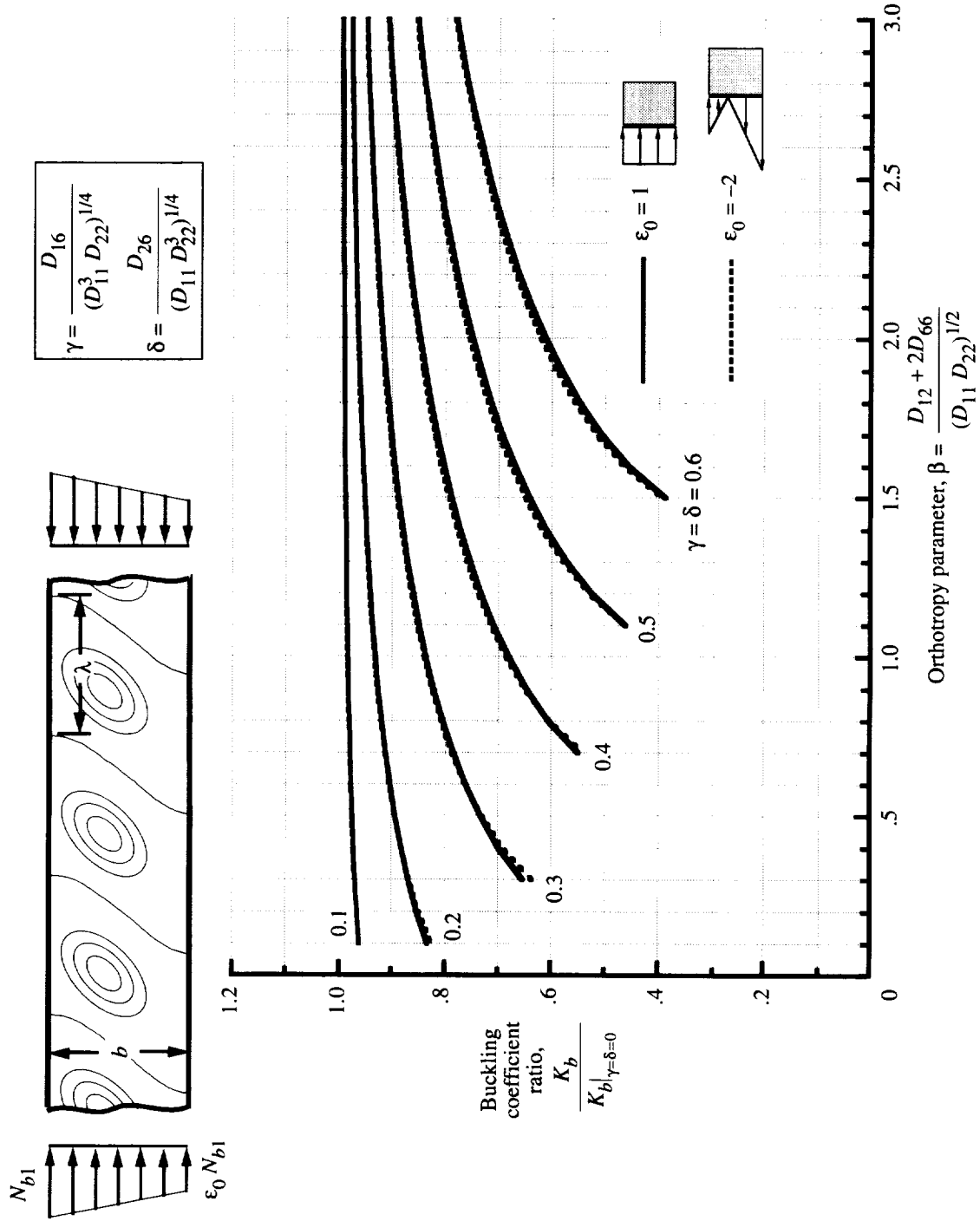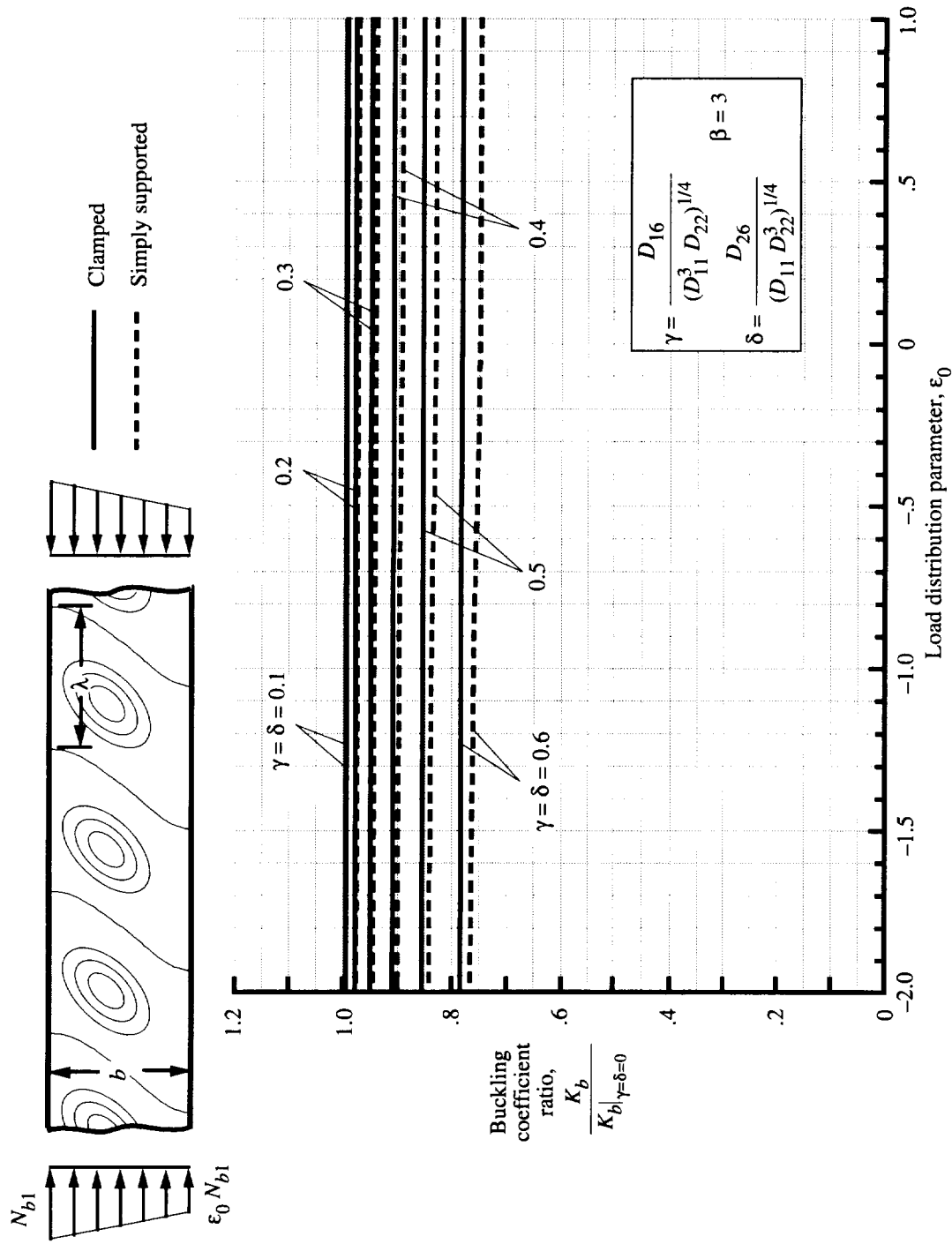
$$\gamma = \frac{D_{16}}{(D_{11}^3\, D_{22})^{1/4}}$$

$$\delta = \frac{D_{26}}{(D_{11}\, D_{22}^3)^{1/4}}$$

Figure 13. Effect of orthotropy parameter β and anisotropy parameters γ and δ on buckling coefficients for clamped plates subjected to linearly varying edge loads.

Buckling coefficient ratio, $\dfrac{K_b}{K_b|_{\gamma=\delta=0}}$

Orthotropy parameter, $\beta = \dfrac{D_{12}+2D_{66}}{(D_{11}\,D_{22})^{1/2}}$

$\gamma = \delta = 0.6$

$\varepsilon_0 = 1$

$\varepsilon_0 = -2$

Figure 14. Effect of load distribution parameter ε_0 and anisotropy parameters γ and δ on buckling coefficients for plates subjected to linearly varying edge loads ($\beta = 3$).
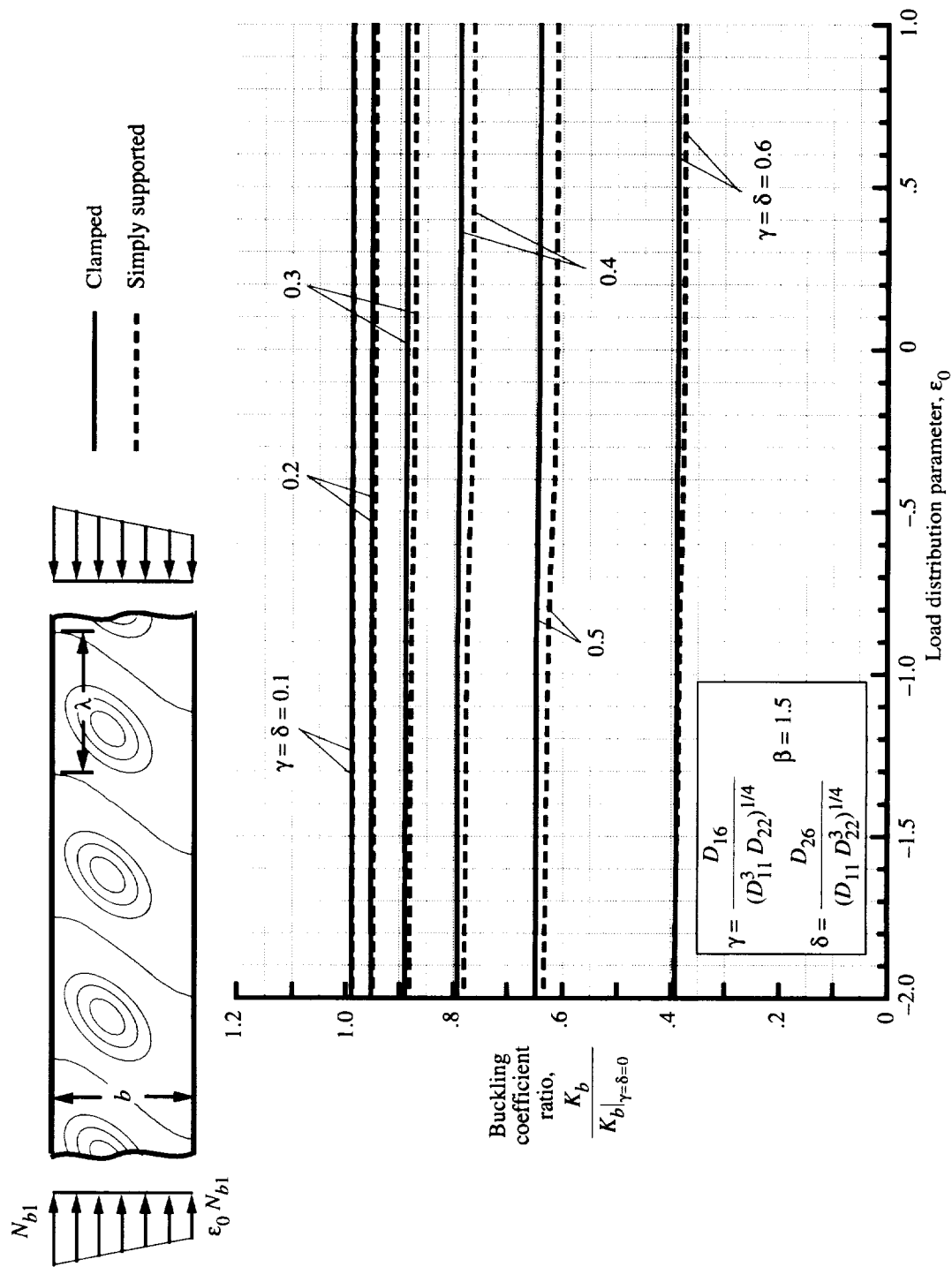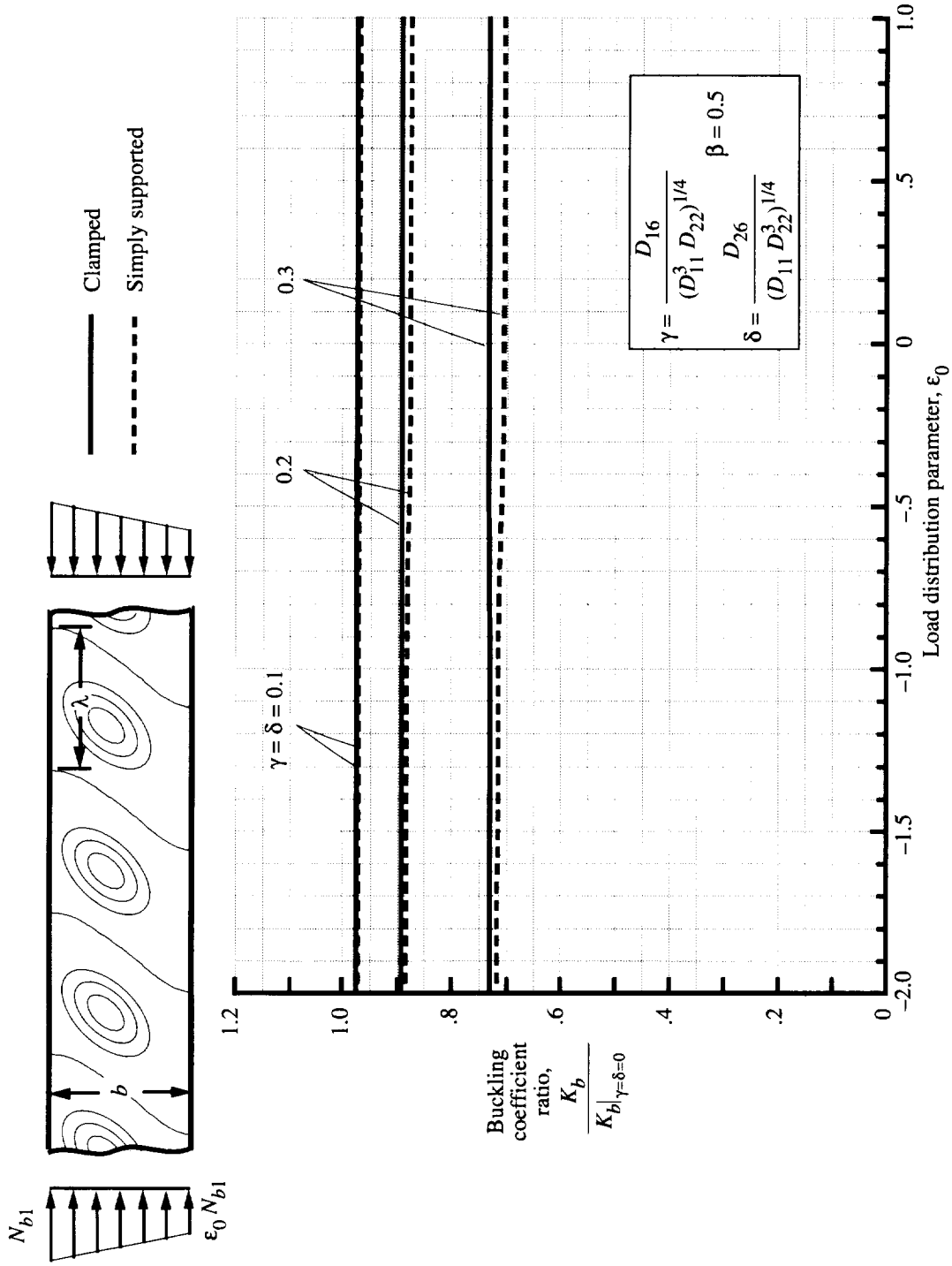
25

Figure 15. Effect of load distribution parameter ε_0 and anisotropy parameters γ and δ on buckling coefficients for plates subjected to linearly varying edge loads ($\beta = 1.5$).
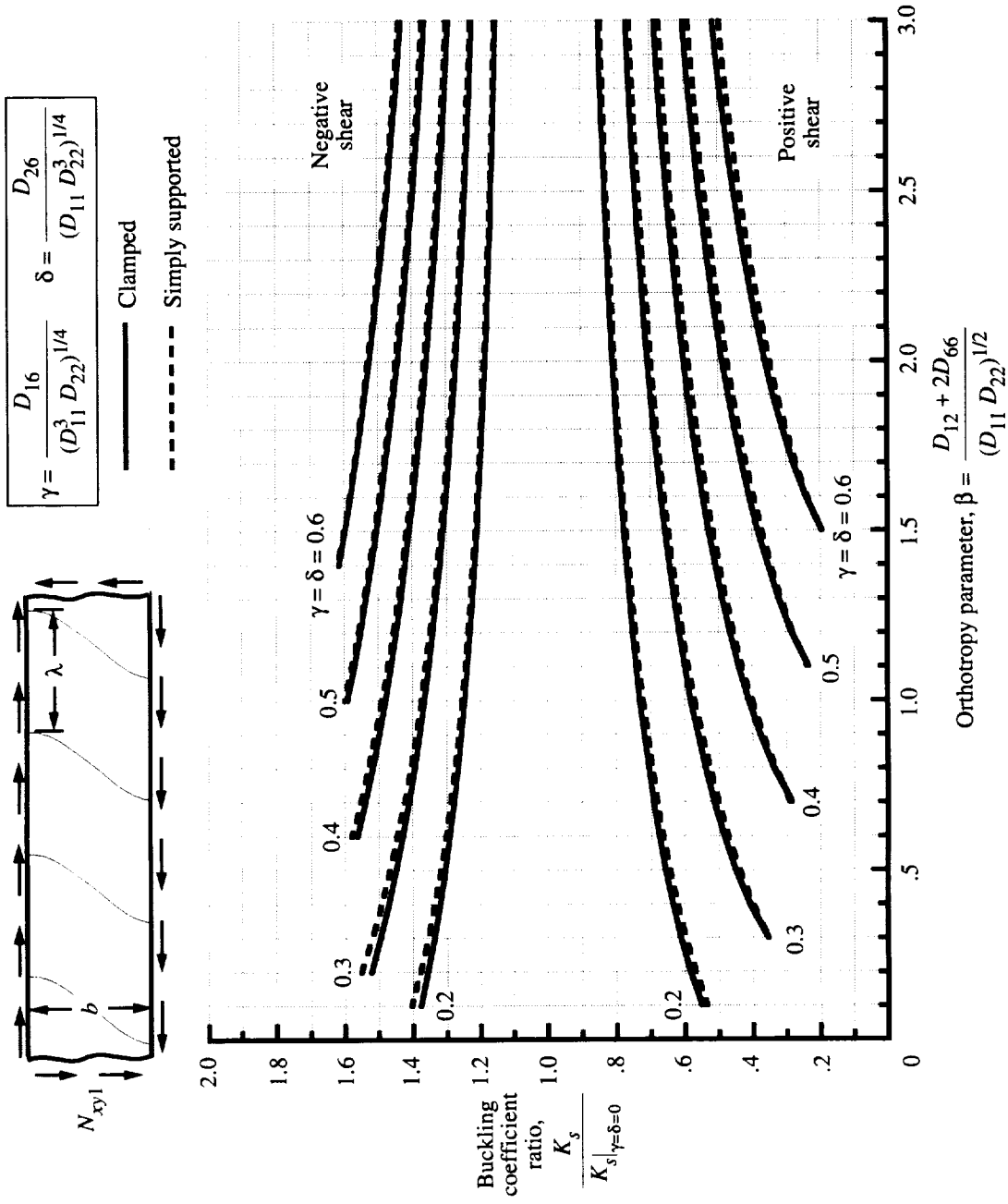
26

Figure 16. Effect of load distribution parameter ε_0 and anisotropy parameters γ and δ on buckling coefficients for plates subjected to linearly varying edge loads ($\beta = 0.5$).

27

Figure 17. Effect of orthotropy parameter β and anisotropy parameters γ and δ on buckling coefficients for plates subjected to shear loads.
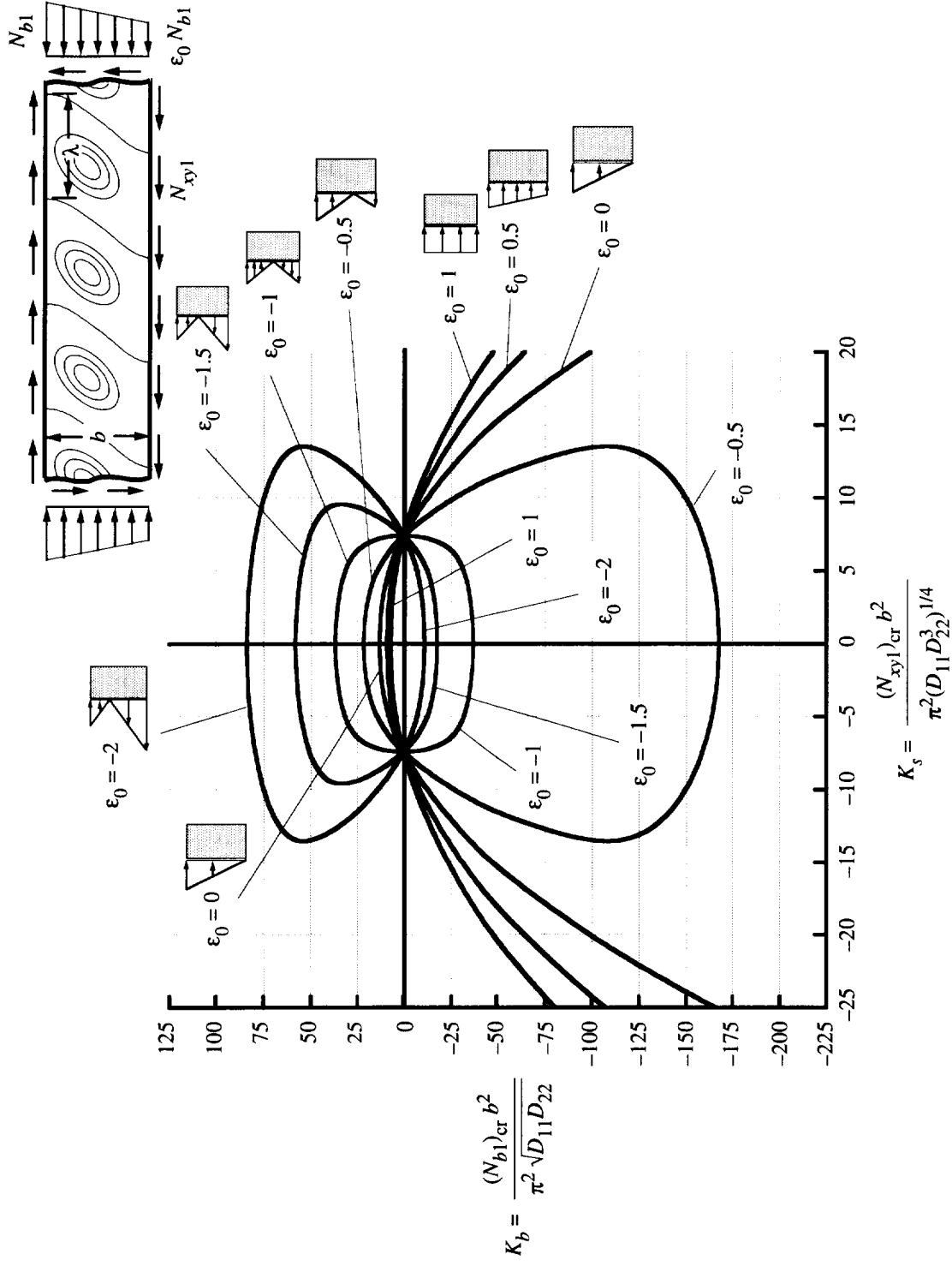
Figure 18. Effect of load distribution parameter ϵ_0 on buckling interaction curves for $[\pm 45]_s$ simply supported plates subjected to linearly varying edge loads and shear loads (anisotropy neglected).

$$K_s = \frac{(N_{xy1})_{cr}\, b^2}{\pi^2 (D_{11}D_{22}^3)^{1/4}}$$

$$K_b = \frac{(N_{b1})_{cr}\, b^2}{\pi^2 \sqrt{D_{11}D_{22}}}$$
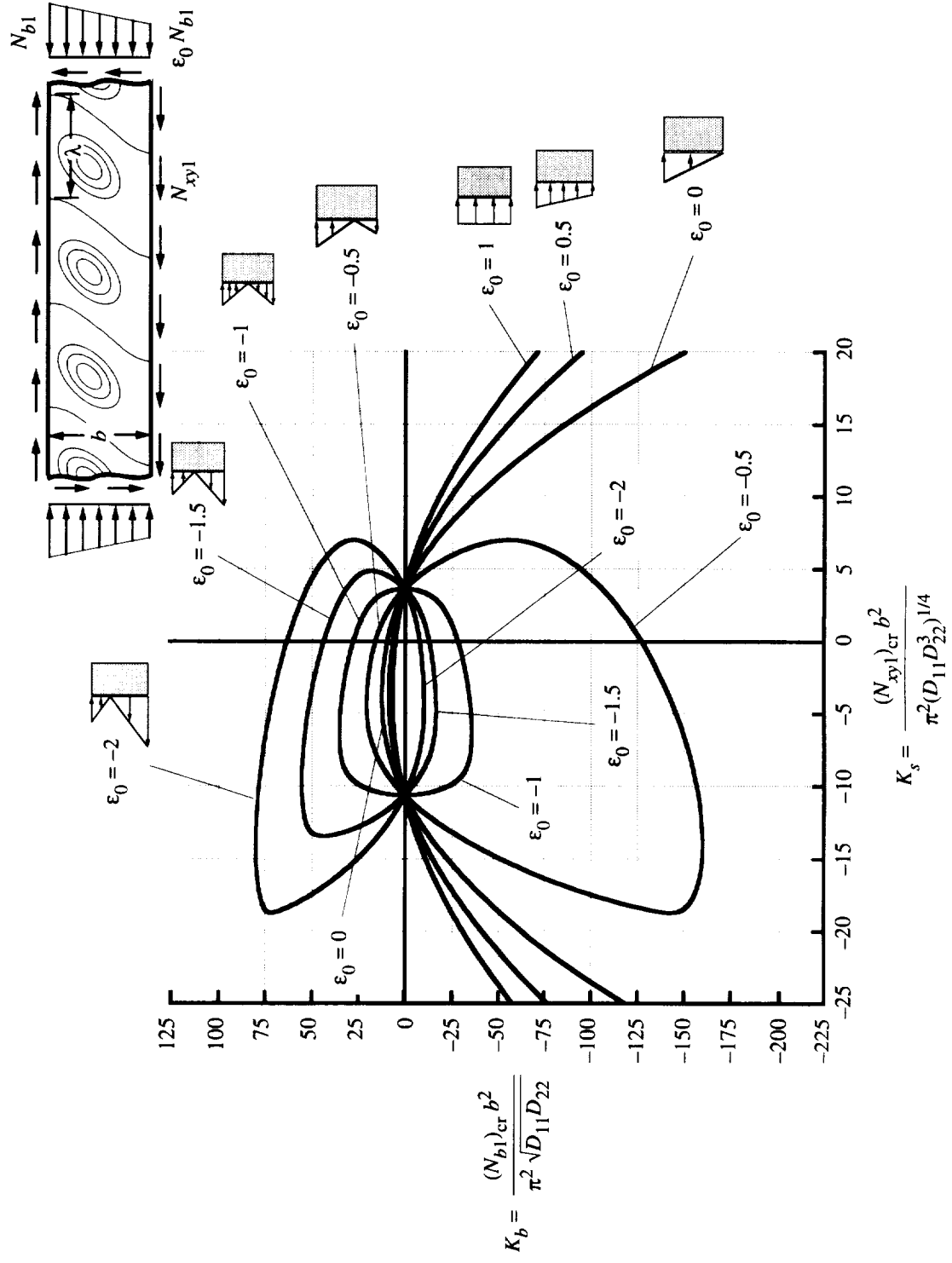
Figure 19. Effect of load distribution parameter ε_0 on buckling interaction curves for $[\pm 45]_s$ simply supported plates subjected to linearly varying edge loads and shear loads (anisotropy included).
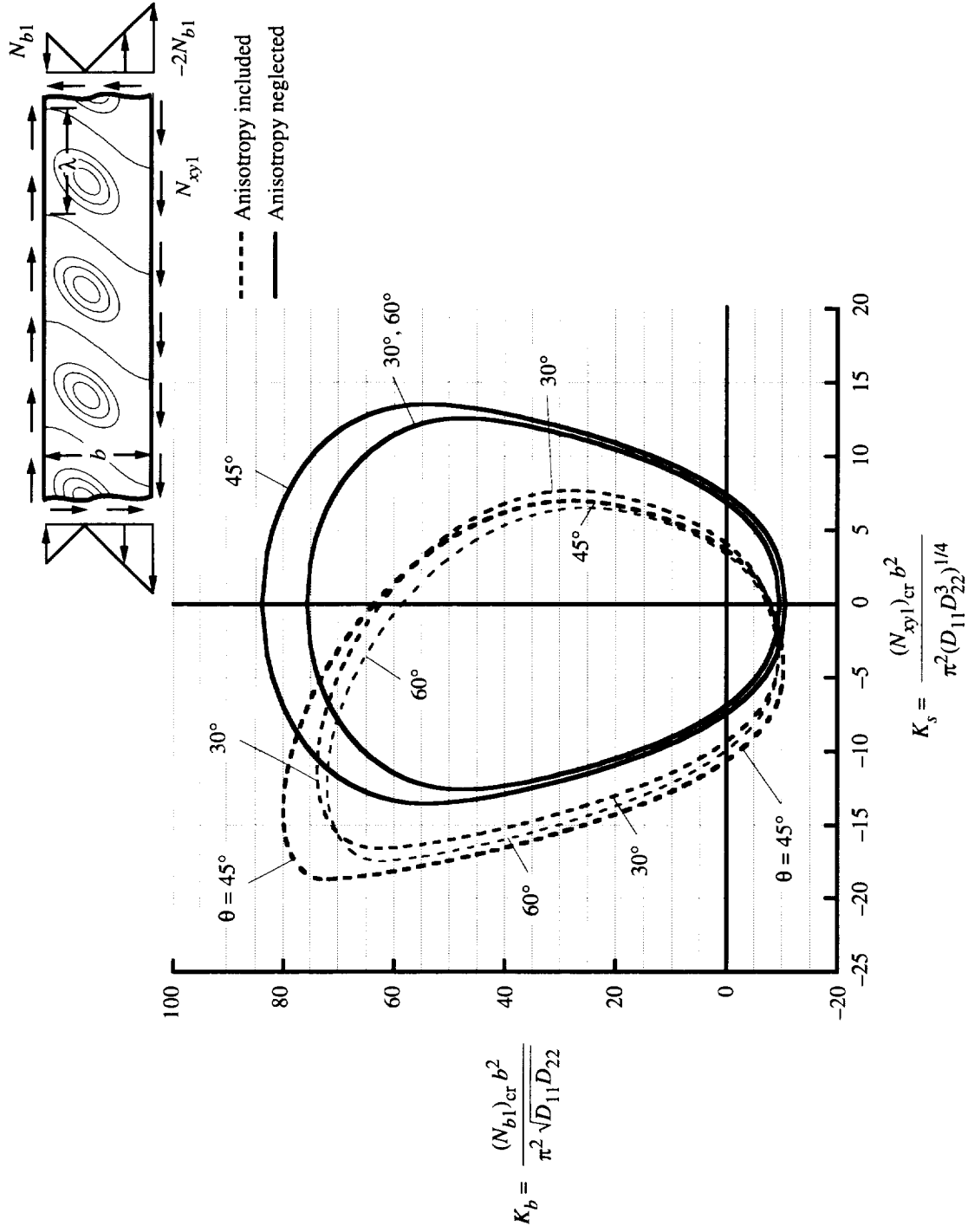
$$K_s = \frac{(N_{xy1})_{cr}\, b^2}{\pi^2 (D_{11} D_{22}^3)^{1/4}}$$

$$K_b = \frac{(N_{b1})_{cr}\, b^2}{\pi^2 \sqrt{D_{11} D_{22}}}$$

30

Figure 20. Importance of anisotropy on buckling interaction curves for $[\pm\theta]_s$ simply supported plates subjected to linearly varying edge loads ($\varepsilon_0 = -2$) and shear loads.
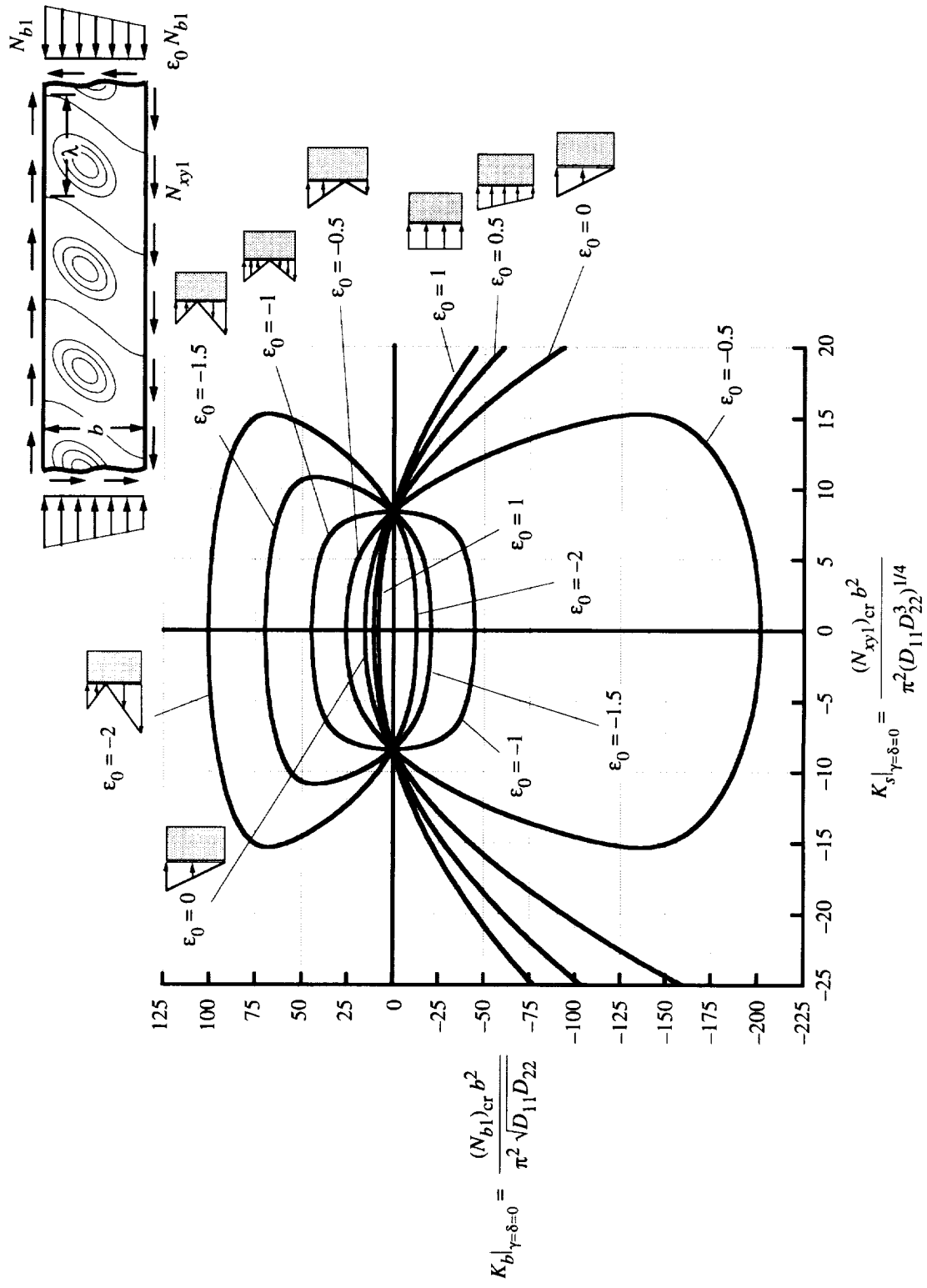
31

Figure 21. Effect of load distribution parameter ε_0 on buckling interaction curves for simply supported specially orthotropic plates subjected to shear and linearly varying edge loads ($\beta = 3$).
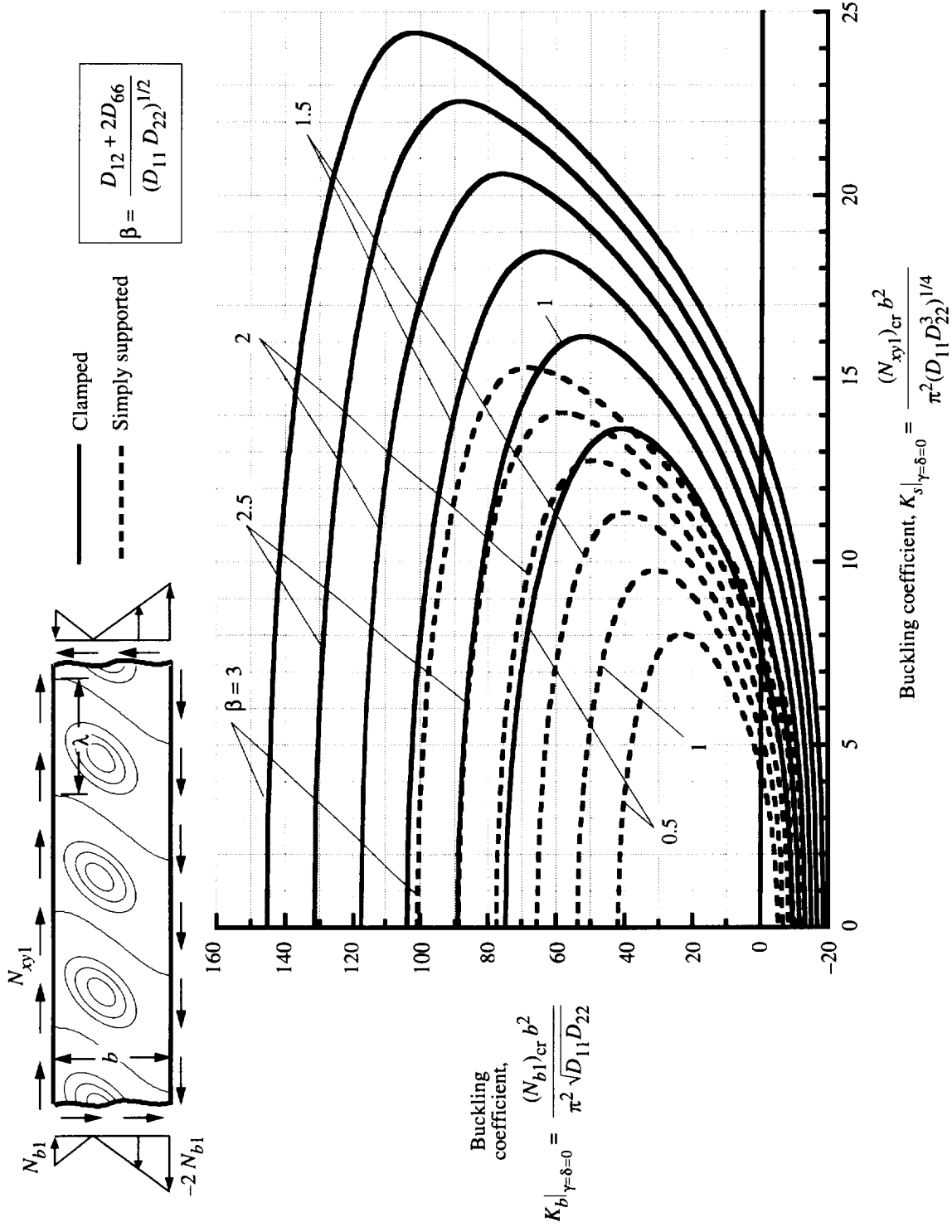
$$K_b\big|_{\gamma=\delta=0} = \frac{(N_{b1})_{\text{cr}}\, b^2}{\pi^2 \sqrt{D_{11} D_{22}}}$$

$$K_s\big|_{\gamma=\delta=0} = \frac{(N_{xy1})_{\text{cr}}\, b^2}{\pi^2 (D_{11} D_{22}^3)^{1/4}}$$

Figure 22. Effect of orthotropy parameter β on buckling interaction curves for specially orthotropic plates (γ = δ = 0) subjected to shear and linearly varying edge loads (ε₀ = −2).

33

$$\beta = \frac{D_{12} + 2D_{66}}{(D_{11}D_{22})^{1/2}}$$

Clamped

Simply supported

N_{xy1}

$-1.5\,N_{b1}$

N_{b1}

$\beta = 3$

2.5

2

1.5

1

0.5

1

Buckling
coefficient,

$$K_b|_{\gamma=\delta=0} = \frac{(N_{b1})_{cr}\,b^2}{\pi^2\,\sqrt{D_{11}D_{22}}}$$

120

100

80

60

40

20

0

-20

0

5

10

15

20

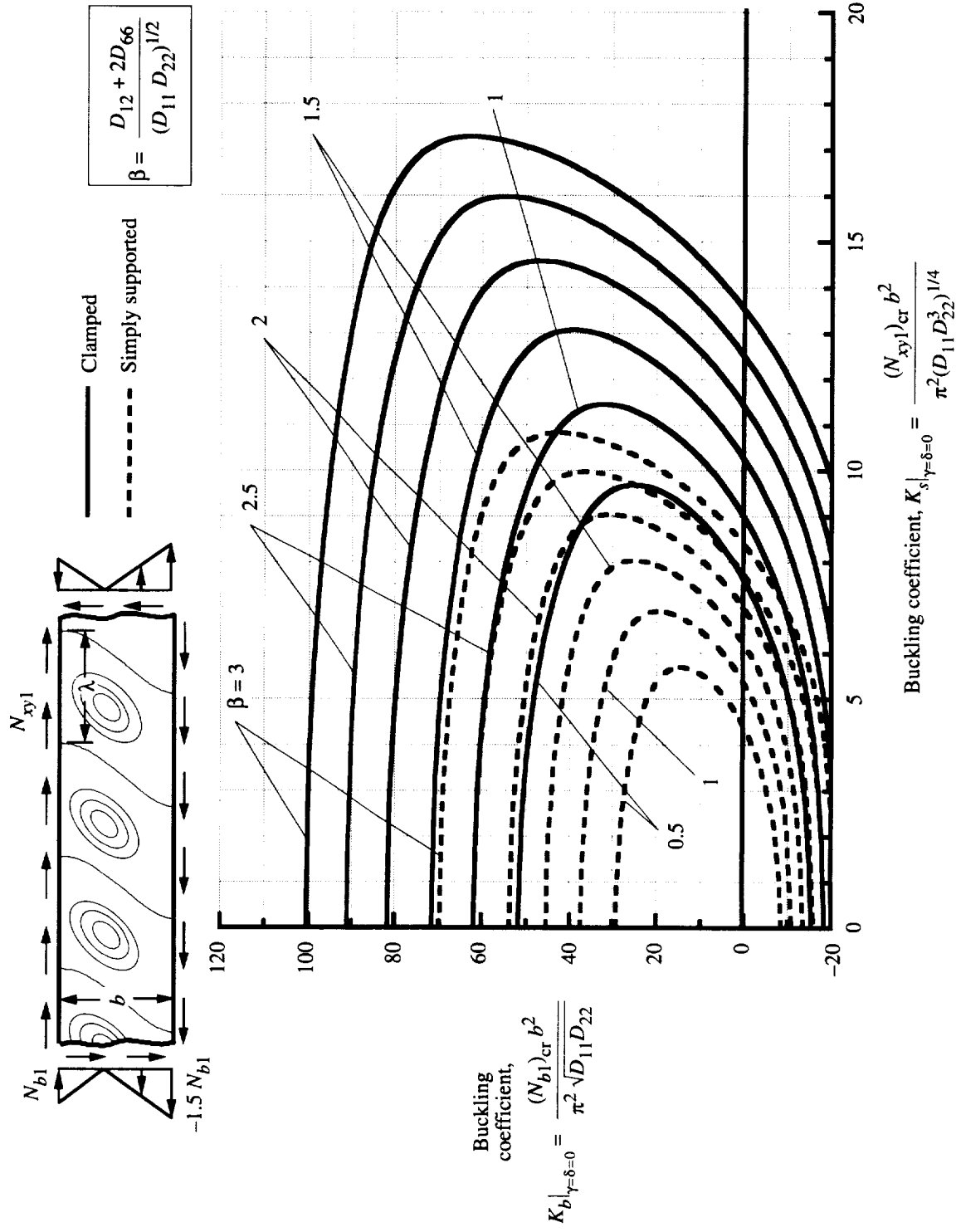Buckling coefficient, $K_s|_{\gamma=\delta=0} = \dfrac{(N_{xy1})_{cr}\,b^2}{\pi^2(D_{11}D_{22}^3)^{1/4}}$

Figure 23. Effect of orthotropy parameter β on buckling interaction curves for specially orthotropic plates ($\gamma = \delta = 0$) subjected to shear and linearly varying edge loads ($\varepsilon_0 = -1.5$).
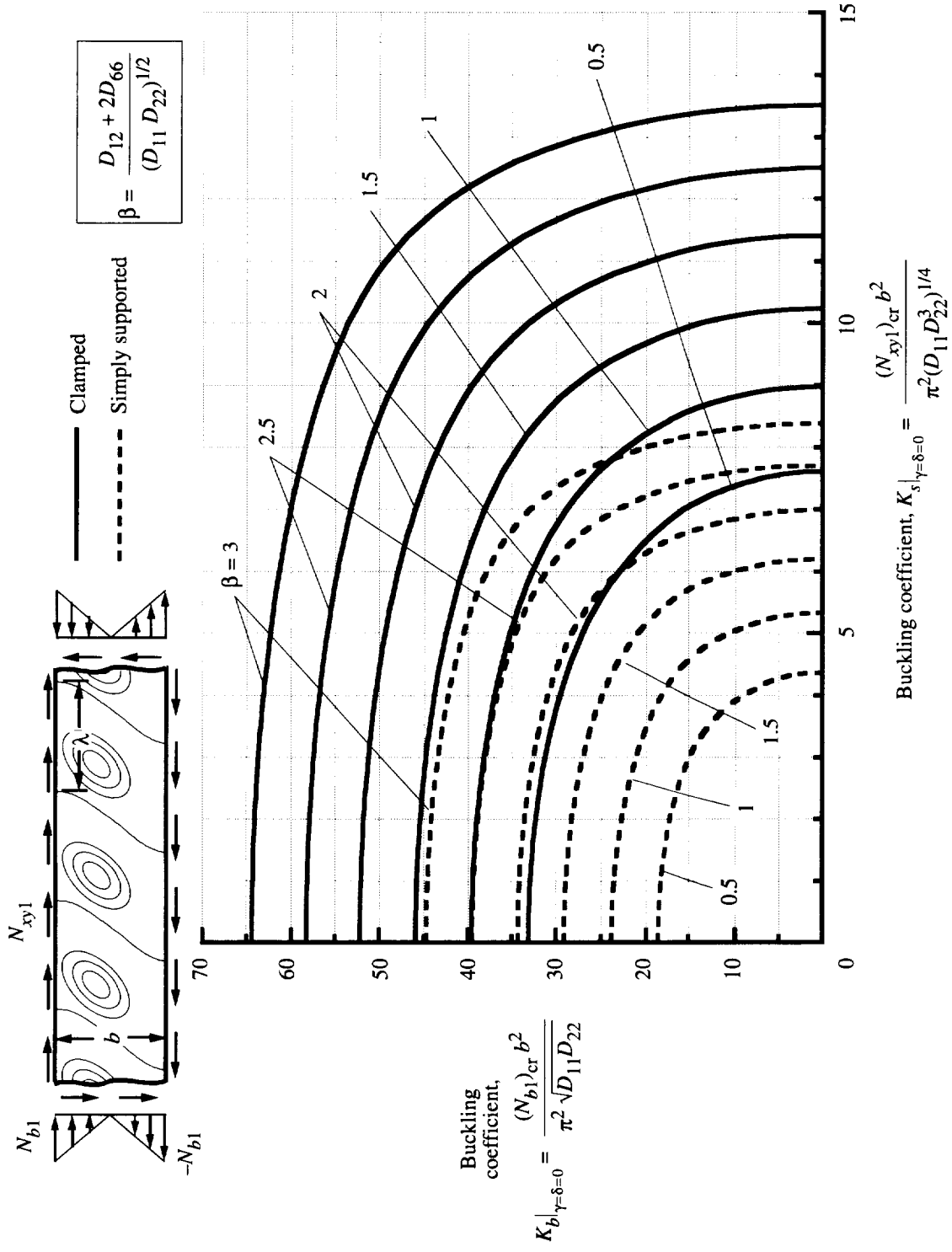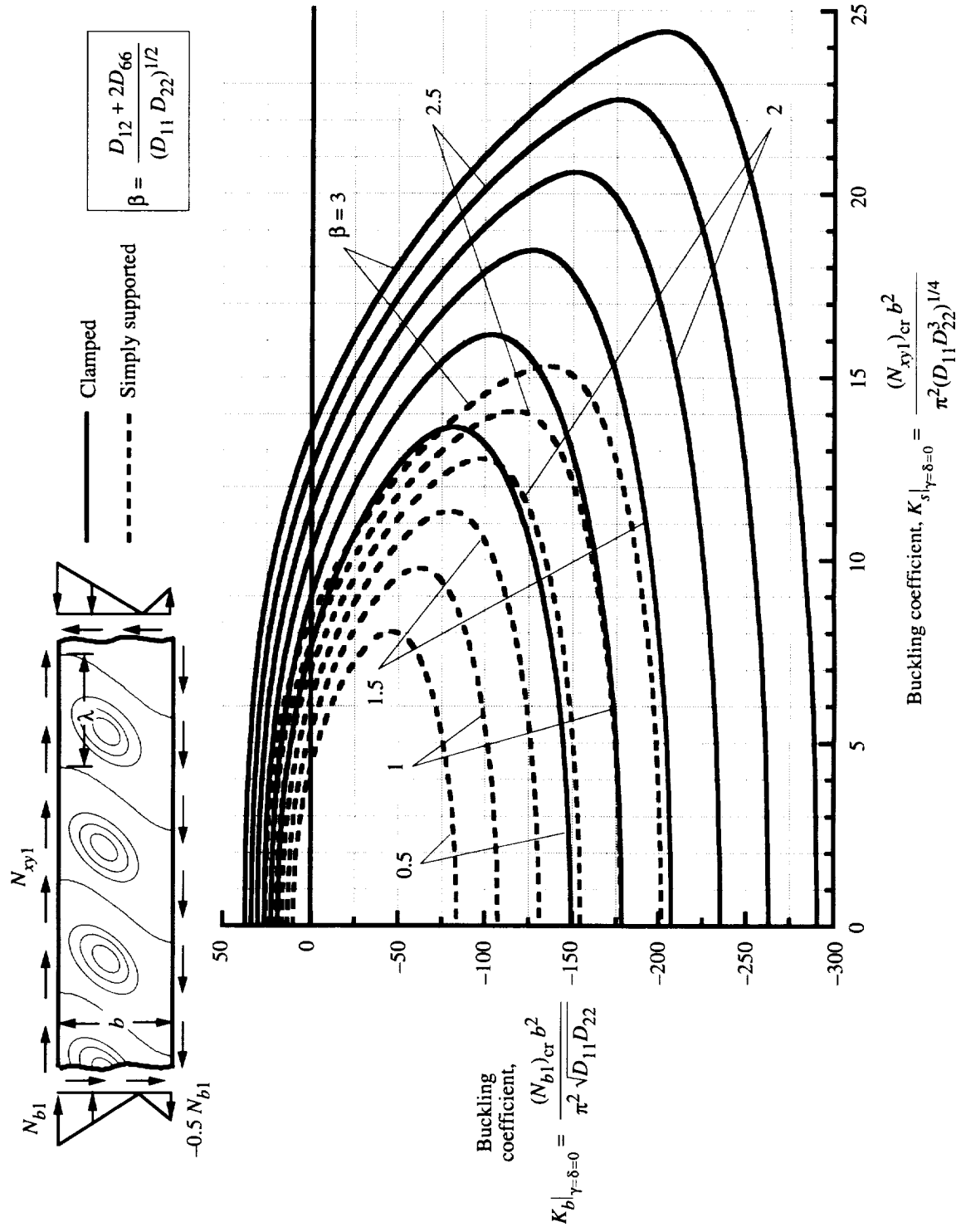
Figure 24. Effect of orthotropy parameter β on buckling interaction curves for specially orthotropic plates ($\gamma = \delta = 0$) subjected to shear and linearly varying edge loads ($\varepsilon_0 = -1$).

$$\beta = \frac{D_{12} + 2D_{66}}{(D_{11}\,D_{22})^{1/2}}$$

——— Clamped

- - - - Simply supported

Buckling coefficient, $K_b|_{\gamma=\delta=0} = \dfrac{(N_{b1})_{cr}\,b^2}{\pi^2\,\sqrt{D_{11}D_{22}}}$

Buckling coefficient, $K_s|_{\gamma=\delta=0} = \dfrac{(N_{xy1})_{cr}\,b^2}{\pi^2(D_{11}D_{22}^3)^{1/4}}$

$\beta = 3$

2.5

2

1.5

1

0.5

Figure 25. Effect of orthotropy parameter β on buckling interaction curves for specially orthotropic plates ($\gamma = \delta = 0$) subjected to shear and linearly varying edge loads ($\varepsilon_0 = -0.5$).
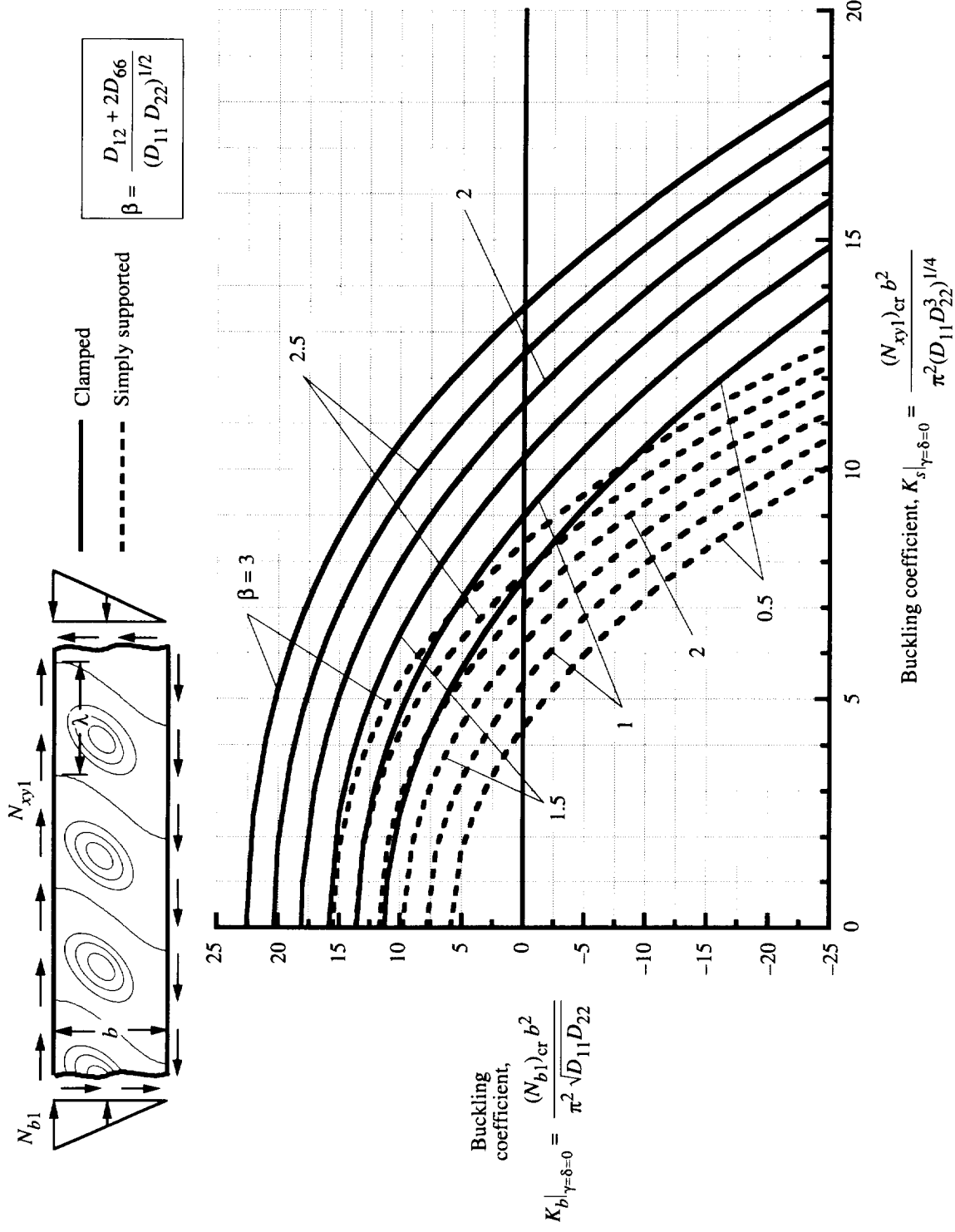
Figure 26. Effect of orthotropy parameter β on buckling interaction curves for specially orthotropic plates ($\gamma = \delta = 0$) subjected to shear and linearly varying edge loads ($\varepsilon_0 = 0$).
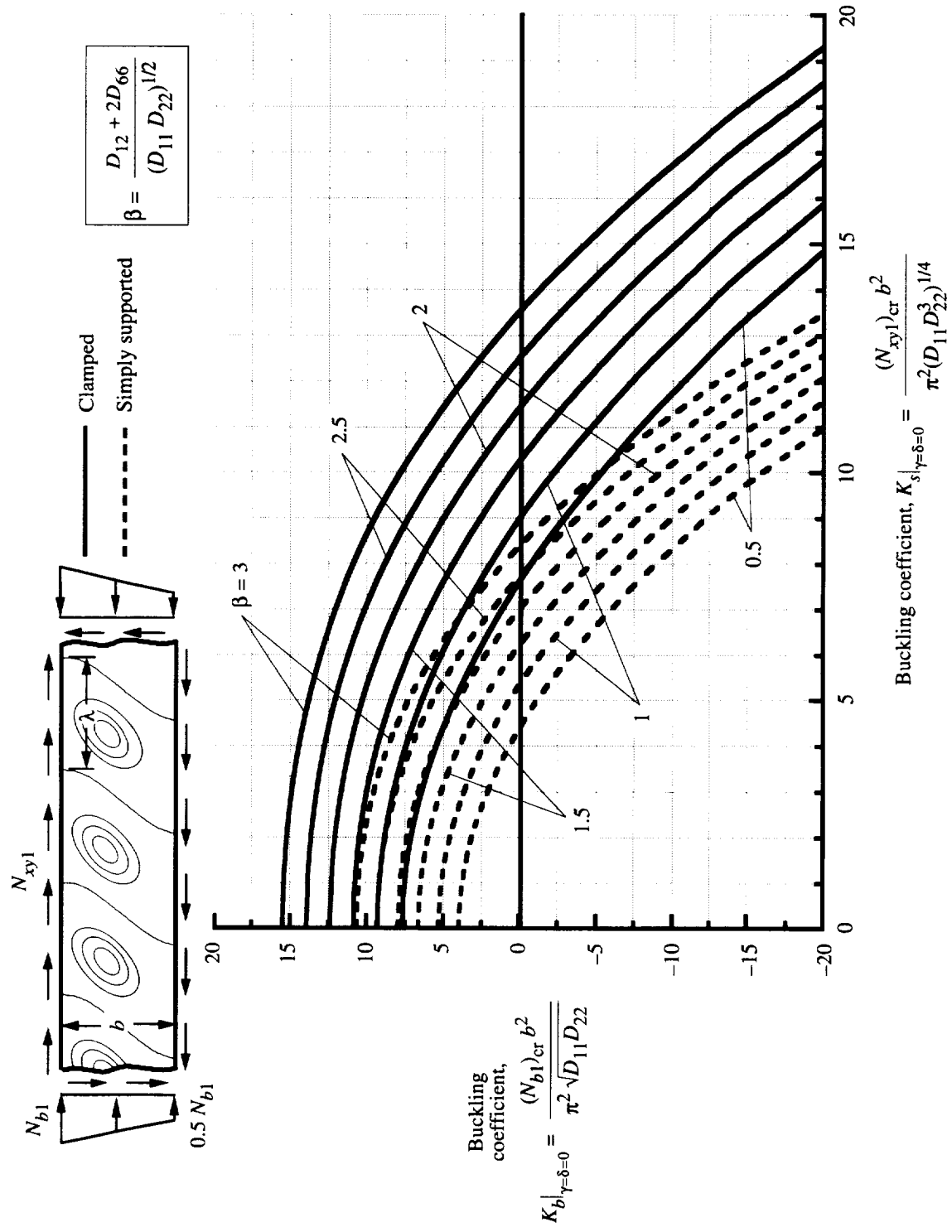
37

Figure 27. Effect of orthotropy parameter β on buckling interaction curves for specially orthotropic plates ($\gamma = \delta = 0$) subjected to shear and linearly varying edge loads ($\epsilon_0 = 0.5$).
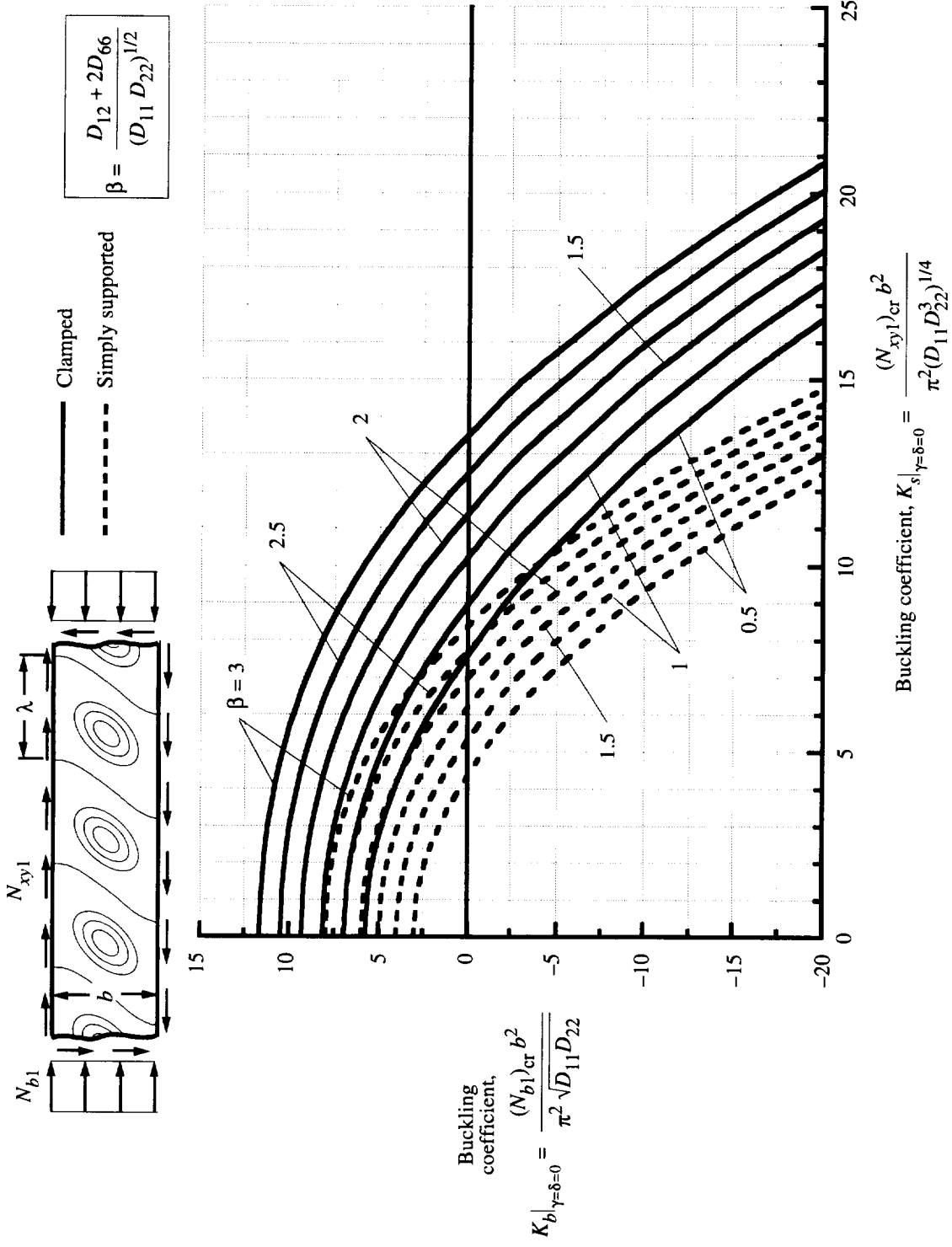
Figure 28. Effect of orthotropy parameter β on buckling interaction curves for specially orthotropic plates ($\gamma = \delta = 0$) subjected to shear and linearly varying edge loads ($\varepsilon_0 = 1$).
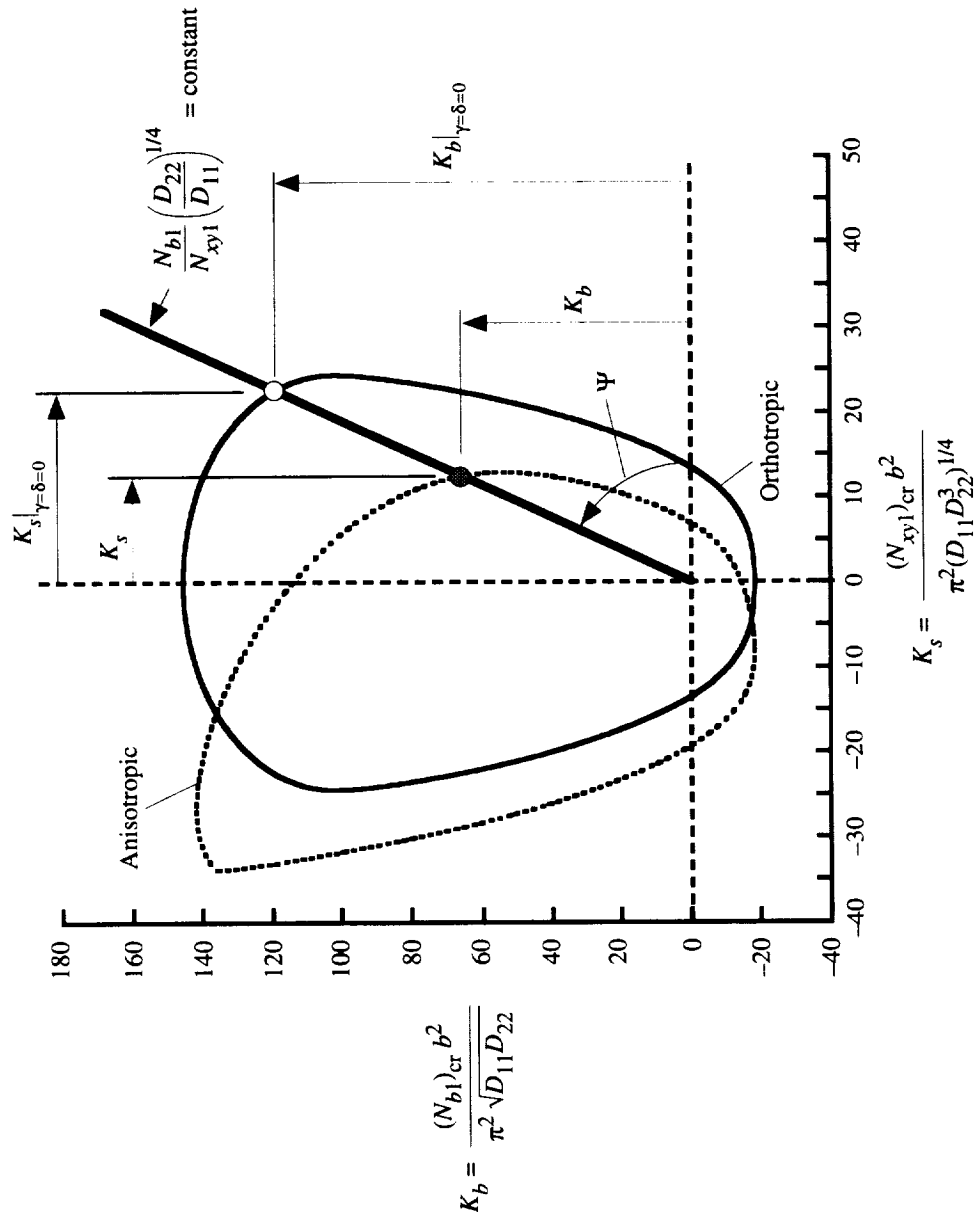
Figure 29. Illustration of stiffness-weighted load ratio angle Ψ for specially orthotropic and anisotropic plates subjected to shear and linearly varying edge loads.
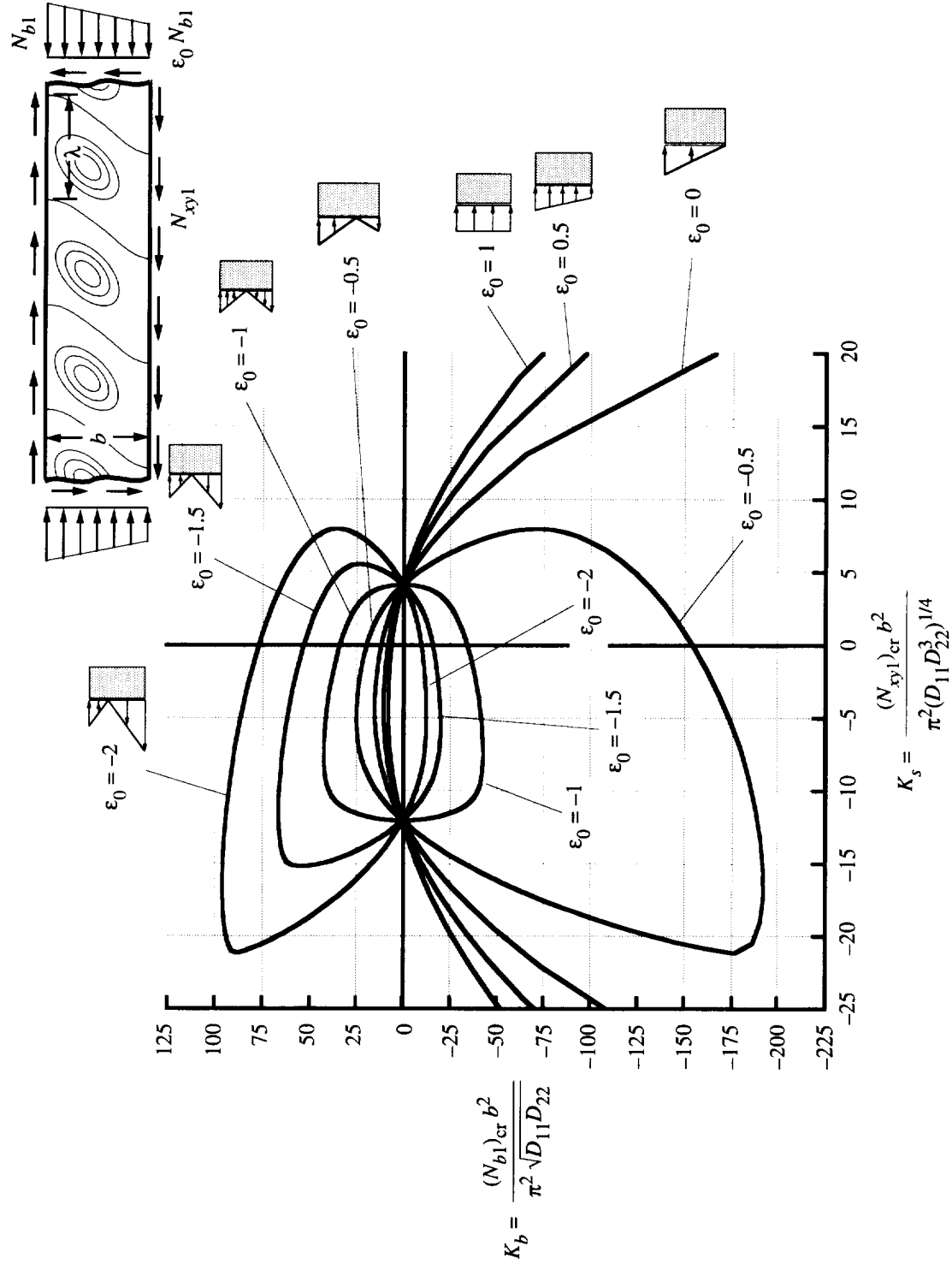
$$\frac{N_{b1}}{N_{xy1}}\left(\frac{D_{22}}{D_{11}}\right)^{1/4} = \text{constant}$$

$$K_s = \frac{(N_{xy1})_{\mathrm{cr}}\, b^2}{\pi^2 (D_{11} D_{22}^3)^{1/4}}$$

$$K_b = \frac{(N_{b1})_{\mathrm{cr}}\, b^2}{\pi^2 \sqrt{D_{11} D_{22}}}$$

40

Figure 30. Effect of load distribution parameter ε_0 on buckling interaction curves for simply supported anisotropic plates subjected to shear and linearly varying edge loads ($\beta = 3$; $\gamma = \delta = 0.6$).
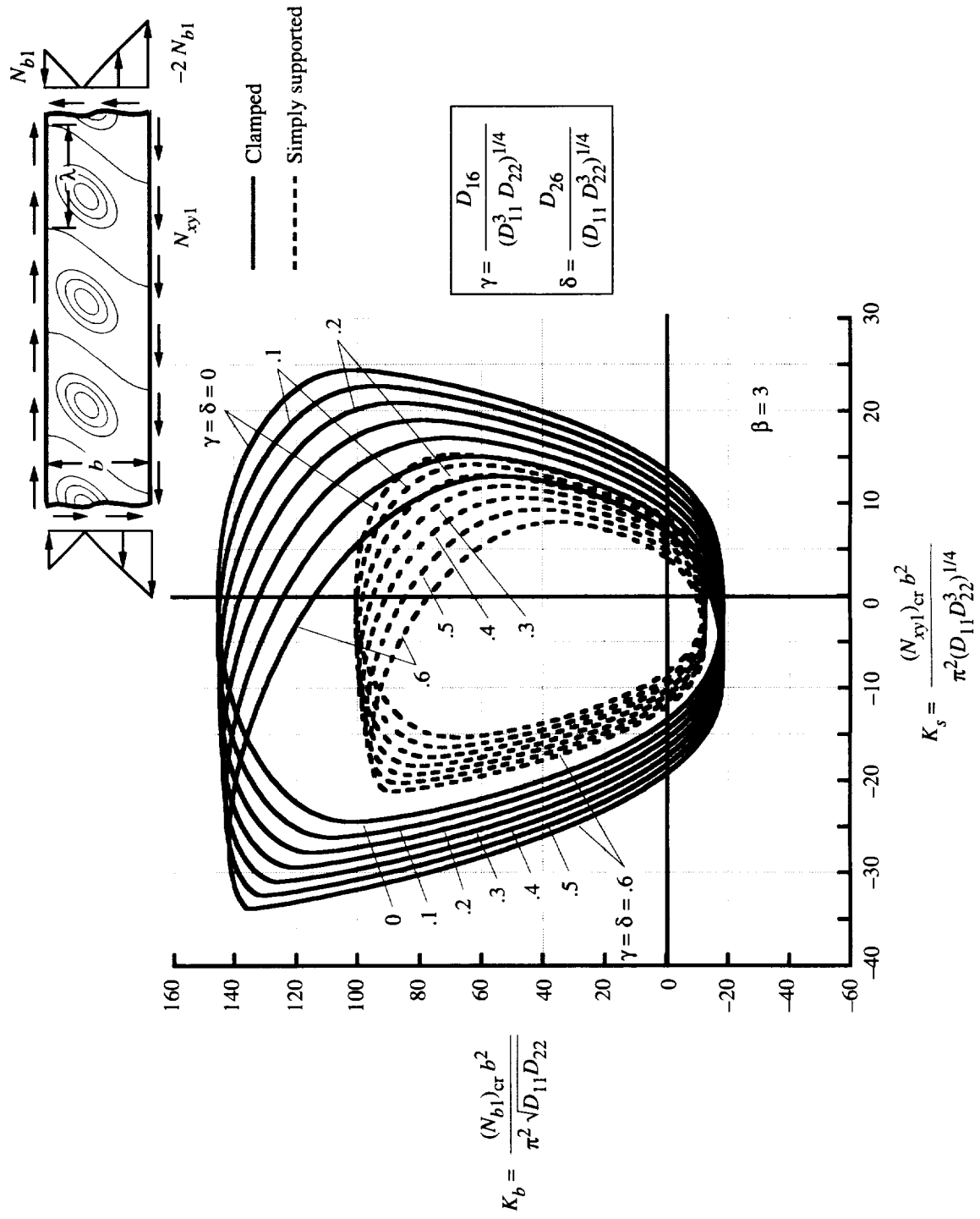
41

Figure 31. Effect of anisotropy parameters γ and δ on buckling interaction curves for plates subjected to shear and linearly varying edge loads ($\beta = 3$; $\varepsilon_0 = -2$).

$$K_b = \frac{(N_{b1})_{cr}\, b^2}{\pi^2 \sqrt{D_{11} D_{22}}}$$

$$K_s = \frac{(N_{xy1})_{cr}\, b^2}{\pi^2 (D_{11} D_{22}^3)^{1/4}}$$

$$\gamma = \frac{D_{16}}{(D_{11}^3\, D_{22})^{1/4}}$$

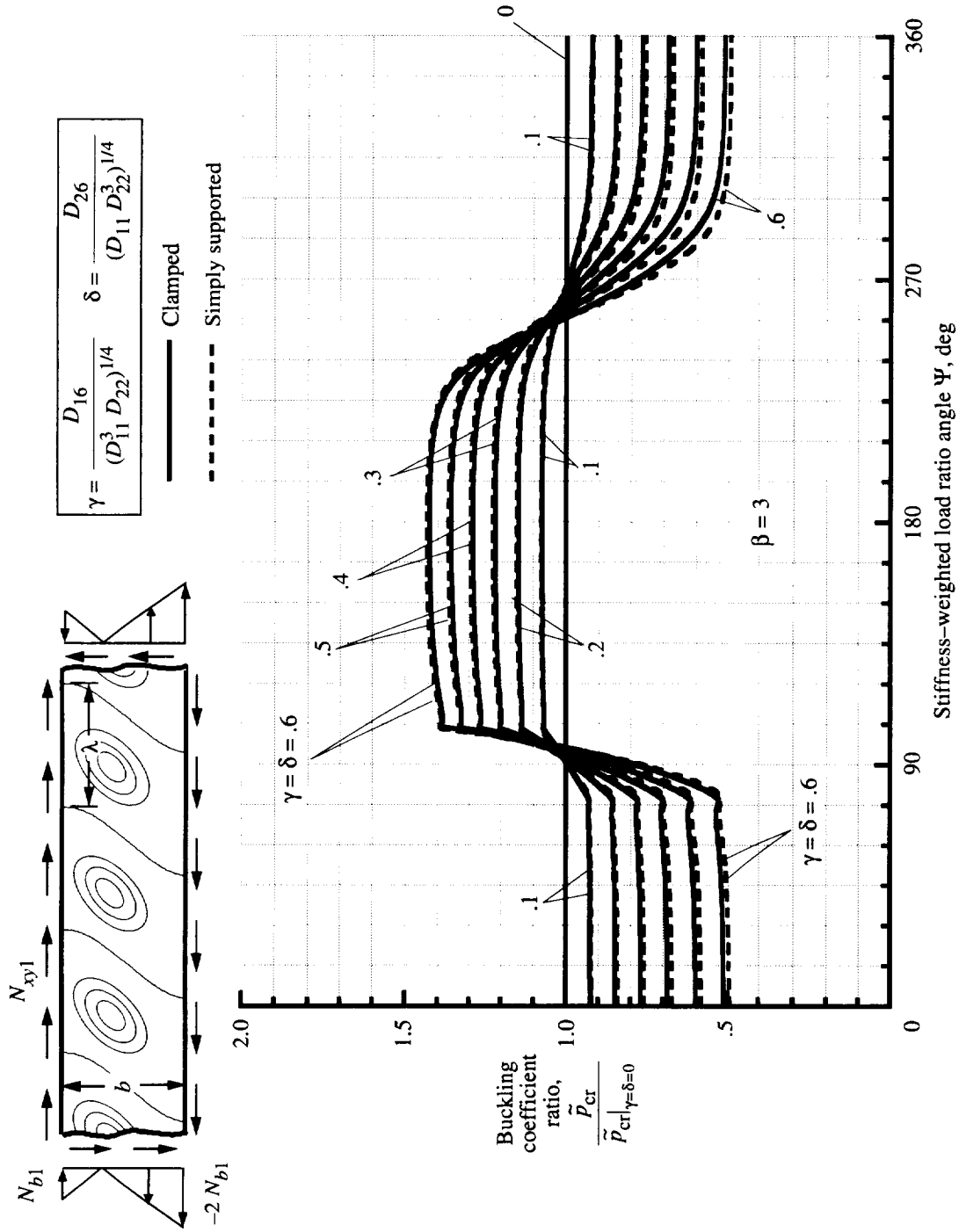$$\delta = \frac{D_{26}}{(D_{11}\, D_{22}^3)^{1/4}}$$

Figure 32. Effect of anisotropy parameters and stiffness-weighted load ratio angle Ψ on behavior of plates subjected to shear and linearly varying edge loads ($\beta = 3$; $\varepsilon_0 = -2$).

43

REPORT DOCUMENTATION PAGE

Form Approved
OMB No. 0704-0188

Public reporting burden for this collection of information is estimated to average 1 hour per response, including the time for reviewing instructions, searching existing data sources, gathering and maintaining the data needed, and completing and reviewing the collection of information. Send comments regarding this burden estimate or any other aspect of this collection of information, including suggestions for reducing this burden, to Washington Headquarters Services, Directorate for Information Operations and Reports, 1215 Jefferson Davis Highway, Suite 1204, Arlington, VA 22202-4302, and to the Office of Management and Budget, Paperwork Reduction Project (0704-0188), Washington, DC 20503.

1. AGENCY USE ONLY *(Leave blank)*	2. REPORT DATE July 1997	3. REPORT TYPE AND DATES COVERED Technical Paper

4. TITLE AND SUBTITLE
Buckling Behavior of Long Symmetrically Laminated Plates Subjected to Shear and Linearly Varying Axial Edge Loads

5. FUNDING NUMBERS
WU 505-63-50-08

6. AUTHOR(S)
Michael P. Nemeth

7. PERFORMING ORGANIZATION NAME(S) AND ADDRESS(ES)

NASA Langley Research Center
Hampton, VA 23681-2199

8. PERFORMING ORGANIZATION REPORT NUMBER

L-17605

9. SPONSORING/MONITORING AGENCY NAME(S) AND ADDRESS(ES)

National Aeronautics and Space Administration
Washington, DC 20546-0001

10. SPONSORING/MONITORING AGENCY REPORT NUMBER

NASA TP-3659

11. SUPPLEMENTARY NOTES
Paper presented at the 11th DoD/NASA/FAA Conference on Fibrous Composites in Structural Design, Ft. Worth, Texas, August 26–30, 1996.

12a. DISTRIBUTION/AVAILABILITY STATEMENT

Unclassified–Unlimited
Subject Category 39
Availability: NASA CASI (301) 621-0390

12b. DISTRIBUTION CODE

13. ABSTRACT *(Maximum 200 words)*

A parametric study of the buckling behavior of infinitely long symmetrically laminated anisotropic plates that are subjected to linearly varying edge loads, uniform shear loads, or combinations of these loads is presented. The study focuses on the effects of the shape of linearly varying edge load distribution, plate orthotropy, and plate flexural anisotropy on plate buckling behavior. In addition, the study examines the interaction of linearly varying edge loads and uniform shear loads with plate flexural anisotropy and orthotropy. Results obtained by using a special purpose nondimensional analysis that is well suited for parametric studies of clamped and simply supported plates are presented for $[\pm\theta]_s$ thin graphite-epoxy laminates that are representative of spacecraft structural components. Also, numerous generic buckling-design charts are presented for a wide range of nondimensional parameters that are applicable to a broad class of laminate constructions. These charts show explicitly the effects of flexural orthotropy and flexural anisotropy on plate buckling behavior for linearly varying edge loads, uniform shear loads, or combinations of these loads. The most important finding of the present study is that specially orthotropic and flexurally anisotropic plates that are subjected to an axial edge load distribution that is tension dominated can support shear loads that are larger in magnitude than the shear buckling load.

14. SUBJECT TERMS
Buckling; Combined loads; Anisotropy; Composite plates

15. NUMBER OF PAGES
44

16. PRICE CODE
A03

17. SECURITY CLASSIFICATION OF REPORT Unclassified	18. SECURITY CLASSIFICATION OF THIS PAGE Unclassified	19. SECURITY CLASSIFICATION OF ABSTRACT Unclassified	20. LIMITATION OF ABSTRACT

NSN 7540-01-280-5500

Standard Form 298 (Rev. 2-89)
Prescribed by ANSI Std. Z39-18
298-102